

FEM analysis for WEDM process

A Thesis Submitted in Partial Fulfillment

For the Requirement for the Degree of

Master of Technology

In

Production Engineering

By

BUDHRAM BOIPAI



Department of Mechanical Engineering

National Institute of Technology

Rourkela –769008

2014

FEM analysis for WEDM process

A Thesis Submitted in Partial Fulfillment

For the Requirement for the Degree of

Master of Technology

In

Production Engineering

By

BUDHRAM BOIPAI

Under the guidance of

Dr. S. S. MAHAPATRA

Professor, Department of Mechanical Engineering



Department of Mechanical Engineering

National Institute of Technology

Rourkela – 769008

2014



National Institute of Technology, Rourkela

CERTIFICATE

This is to certify that the thesis entitled, “**FEM analysis for WEDM process**” submitted by Budhram Boipai in partial fulfillment of the requirements for the award of Master of Technology Degree in Mechanical Engineering with specialization in Production Engineering at the National Institute of Technology, Rourkela is an authentic work carried out by him under my supervision and guidance.

To the best of my knowledge, the matter embodied in the thesis has not submitted to any other University/Institute for the award of any degree or diploma.

Date:

Dr. S. S. Mahapatra

Dept. of Mechanical Engineering

National Institute of Technology

Rourkela – 769008

ACKNOWLEDGEMENT

I would like to express my deep sense of respect and gratitude toward my supervisor **Dr. S. S. Mahapatra**, who not only guided the academic project work but also stood as a teacher and philosopher in realizing the imagination in pragmatic way, I want to thank him for introducing me for the field of Optimization and giving the opportunity to work under him. His presence and optimism have provided an invaluable influence on my career and outlook for the future. I consider it my good fortune to have got an opportunity to work with such a wonderful person.

Date

BUDHRAM BOIPAI

Nomenclature

EDM	Electrical discharge machining
WEDM	Wire Electrical discharge machining
MRR	Material removal rate (mm^3/min)
h_i	heat input to the wire
V	Voltage (V)
I	Current (Ampere)
$q(r)$	Heat flux (W/m^2)
R	Spark radius (μm)
K	Thermal conductivity ($\text{W}/\text{m}\cdot\text{K}$)
T	Temperature variable (K or $^{\circ}\text{C}$)
T_0	Initial temperature (K or $^{\circ}\text{C}$)
t_{on}	Spark-on time (μs)
t_{off}	Spark-off time (μs)
C_p	Specific heat ($\text{J}/\text{kg}\cdot\text{K}$)

Abstract

Wire electrical discharge machining (WEDM) is widely used in machining of conductive materials when precision is considered as a prime importance. This work proposes a three dimensional finite element model (using ANSYS software) and new approach to predict the temperature distribution at different pulse time as well as stress distribution in wire. A transient thermal analysis assuming a Gaussian distribution heat source with temperature-dependent material properties has been used to investigate the temperature distribution and stress distribution. Thermal stress developed after the end of the spark and residual stress developed after subsequent cooling. The effect on significant machining parameter pulse-on-time has been investigated and found that the peak temperature sharply increases with the parameter.

Keywords: ANSYS, WEDM, Residual stress, Thermal stress, Temperature

CHAPTER	CONTENTS	PAGE NOS.
	CERTIFICATE	iii
	ACKNOWLEDGEMENT	iv
	NOMENCLATURE	v
	ABSTRACT	vi
	CHAPTERS.....	vii-viii
	LIST OF FIGURE.....	ix
	LIST OF TABLE.....	x
Chapter 1		(Pages 1-7)
	1 INTRODUCTION.....	1
	1.1 Research Background.....	2
	1.1.1 WEDM process.....	4
	1.1.2 Principle of spark erosion.....	5
	1.1.3 Terms used in WEDM process.....	6
	1.1.4 The use of Dielectric in WEDM Process.....	6
	1.1.5 WEDM applications in industry.....	7
	1.2 Objective of the Present Research Work.....	7
Chapter 2		(Pages 8-17)
	2 LITERATURE REVIEW.....	8
Chapter 3		
	3 Modelling procedure using ANSYS of WEDM	19
	3.1 Thermal model of Wire EDM.....	19
	3.1.1 Assumption.....	19

3.1.2 Thermal Model	20
3.1.3 Governing equation	20
3.1.4 Boundary conditions.....	21
3.1.5 Material properties.....	22
3.1.6 Heat Flux due to the wire electrode in a single spark.....	23
3.1.7 Spark Radius.....	23
3.2 Finite Element Analysis Procedure using ANSYS software	24
3.2.1 Thermal analysis of brass wire	24
3.2.2 Process of thermo-structural modeling.....	25
Chapter 4	
4.1 ANSYS model confirmation	28
4.2 FEM analysis.....	28
4.2.1 Thermal modeling of wire EDM for single spark in brass wire.....	28
4.2.2. Structural modeling of WEDM in molybdenum wire.....	33
4.2.3. Thermo-structural analysis of WEDM in brass wire.....	37
4.3 Results and Discussion.....	54
Chapter 5	
5 CONCLUSIONS.....	55
REFERENCES	57

LIST OF FIGURE

FIGURE NOs .	CONTENTS	PAGE NOS.
Figure 1	Schematic diagram of WEDM.....	3
Figure 2	Cutting mechanism in Wire EDM process	4
Figure 3	Sparking phenomena in WEDM process.....	5
Figure 4	Three-dimensional thermal analysis models for WEDM.....	21
Figure 5	Three-dimensional view of the meshed model	25
Figure 6	Temperature distribution in Brass wire with $V=25V$, $I=27 A$, $P=0.38$ and $t_{on}= 0.12\mu s$	30
Figure 7	Temperature distribution in Brass wire with $V=25V$, $I=27 A$, $P=0.38$ and $t_{on}= 0.26\mu s$	30
Figure 8	Temperature distribution in Brass wire with $V=25V$, $I=27 A$, $P=0.38$ and $t_{on}= 0.36\mu s$	31
Figure 9	Temperature distribution in Brass wire with $V=25V$, $I=27 A$, $P=0.38$ and $t_{on}= 0.58\mu s$	32
Figure 10	Temperature distribution in Brass wire with $V=25V$, $I=27 A$, $P=0.38$ and $t_{on}= 1.2\mu s$	33
Figure 11	Temperature distribution in Brass wire with $V=25V$, $I=27 A$, $P=0.38$ and $t_{on}= 1.82\mu s$	33
Figure 12	Nodal solution of displacement of molybdenum wire.....	34
Figure 13	Graph of displacement of molybdenum wire.....	35
Figure 14	Thermal stress in X-component at $t_{on}=0.12 \mu s$	36
Figure 15	Thermal stress in Y-component at $t_{on}=0.12 \mu s$	37
Figure 16	Thermal stress in Z-component at $t_{on}=0.12 \mu s$	38
Figure 17	Thermal shear stress in XY-component at $t_{on}=0.12 \mu s$	39
Figure 18	Thermal shear stress in XZ-component at $t_{on}=0.12 \mu s$	40
Figure 19	Thermal shear stress in YZ-component at $t_{on}=0.12 \mu s$	41
Figure 20	Residual stress at $t_{off} = 3\mu s$	42
Figure 21	Thermal stress in X-component at $t_{on}=0.52 \mu s$	43

Figure 22 Thermal stress in Y-component at $t_{on}=0.52 \mu s$	44
Figure 23 Thermal stress in Z-component at $t_{on}=0.52 \mu s$	44
Figure 24 Thermal shear stress in XY-component at $t_{on}=0.52 \mu s$	45
Figure 25 Thermal shear stress in XZ-component at $t_{on}=0.52 \mu s$	46
Figure 26 Thermal shear stress in YZ-component at $t_{on}=0.52 \mu s$	46
Figure 27 Residual stress at $t_{off} = 3\mu s$	47
Figure 28 Thermal stress in X-component at $t_{on}=1.82 \mu s$	48
Figure 29 Thermal stress in Y-component at $t_{on}=1.82 \mu s$	48
Figure 30 Thermal stress in Z-component at $t_{on}=1.82 \mu s$	49
Figure 31 Thermal shear stress in XY-component at $t_{on}=1.82 \mu s$	51
Figure 32 Thermal shear stress in XZ-component at $t_{on}=1.82 \mu s$	52
Figure 33 Thermal shear stress in YZ-component at $t_{on}=1.82 \mu s$	53
Figure 34 Residual stress at $t_{off} = 3\mu s$	54

LIST OF TABLE

TABLE NO.s	CONTENTS	PAGE NO.s
Table 1	Properties of brass wire.....	22
Table 2	Properties molybdenum wire.....	23
Table 3	Parameters used for thermal analysis in WEDM process.....	29
Table 4	Parameters used for structural analysis in WEDM process.....	35

Chapter 1

- **Introduction**

- **Research Background**
- **Objectives of the work**

1.1 Research Background

Wire electrical discharge machining process is a mostly used non-conventional material removal processes. This is use for manufacturing difficult shape and profile of hard materials. This is considering as a distinctive variation of the conventional electrical discharge machining processes. In the WEDM, demand is growing for high rate cutting speed and high accuracy machining for improve the productivity of product and also for achieve high excellence quality in machining job. In wire electrical discharge machining process a always travelling wire electrode made of thin copper, brass or tungsten of diameter 0.05–0.3 mm is used, which is precisely controlled by a CNC system. Here role of CNC is very important. The function of CNC is unwind the wire from a first spool, and feed throughout the work-piece, and takes it on a second spool. Generally wire velocity varies from 0.1 to 10 m/min, and feed rate is 2 to 6 mm/min. A direct current is used for generate high frequency pulse to the wire and the workpiece. The wire (electrode) is hold in tensioning device for decreases the chance of producing inaccurate parts. In wire electrical machining process, the workpiece and tool is eroded and there is no direct contact between the workpiece and the electrode, and this reduces the stress during machining.

WEDM was initially developed by manufacturing industry in the since 1960. The development technique is replaced the machined electrode used in electrical discharge machining. In 1974, D.H. Dulebohn introduced the optical line follower system which is automatic control the shapes of the part to be machined by the wire electrical discharge machining process. In 1975, it was popular rapidly, and its capability was better understood by manufacturing industry. When the computer numerical control system was introduced in WEDM process this brought about a most important development of the machining process.

Consequently the wide capability of the wire electrical discharge machining process was widely exploited for any through-hole machining owing to the wire, which has to pass through the part to be machined. The common application of wire electrical discharge machining process is the fabricate the stamp and extrusion tools and dies, fixtures and gauges, prototypes, aircraft and medical parts, and grinding wheel form tools. The symmetric diagram of WEDM is as shown Fig.1.

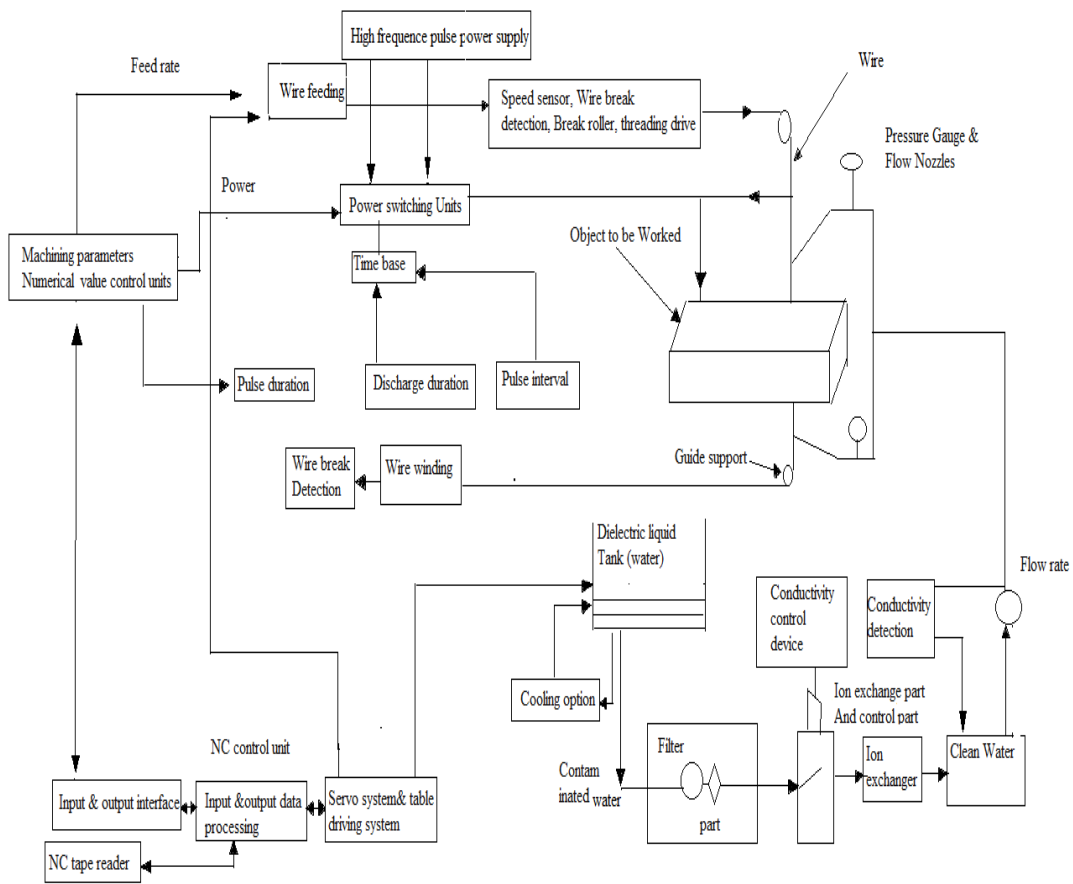


Fig. 1: Schematic diagram of WEDM (Source: Datta and Mahapatra, [1])

1.1.1 Wire-EDM process

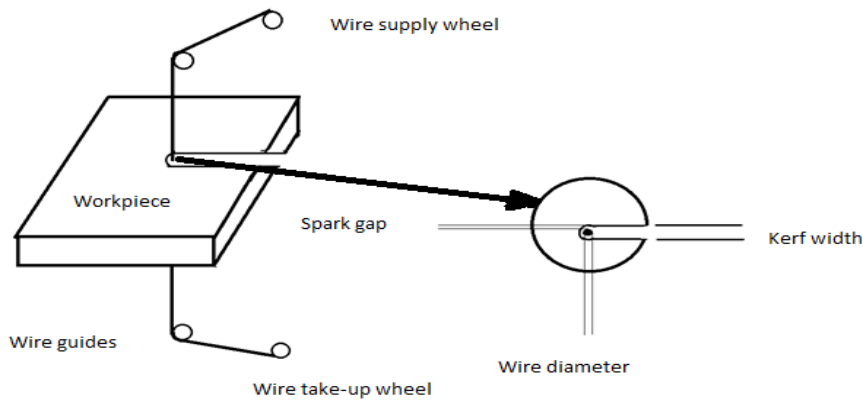


Fig.2. WEDM process (Source: Datta and Mahapatra, [1])

The method of material removal in wire electrical machining is as like to the conventional electrical discharge machining process concerning the erosion effect on workpiece by the spark. In wire electrical discharge machining, material is eroded from the workpiece by a cycle of spark occur between workpiece and wire which is separate by dielectric liquid, which is continuously fed to the machining zone. But now-a-days, wire electrical discharge machining process is commonly conducted in fully submerge container fill with dielectric liquid. This type of submerge method of wire electrical discharge machining promote temperatures stabilization and efficient flushing in case where the workpiece has variation in thickness. The wire electrical discharge machining process generally use of electrical energy generate the plasma channel between the cathode and anode and create thermal energy at a temperature in the range between $8,000^{\circ}\text{C}$ to $12,000^{\circ}\text{C}$ or as higher as $20,000^{\circ}\text{C}$ and create considerable amount of heat and melting of the materials on the surfaces of each pole. When the pulsating direct current power supplying occurs between 20,000 and 30,000 Hz is turned off, the plasma channel breaks down. This cause sudden decrease in the temperature, allow circulate dielectric liquid to implore the

plasma channel and flushing the molten particle from the each pole surface in the form of microscopic debris. The WEDM machining process is as shown in Fig. 2.

1.1.2 Principle of spark erosion

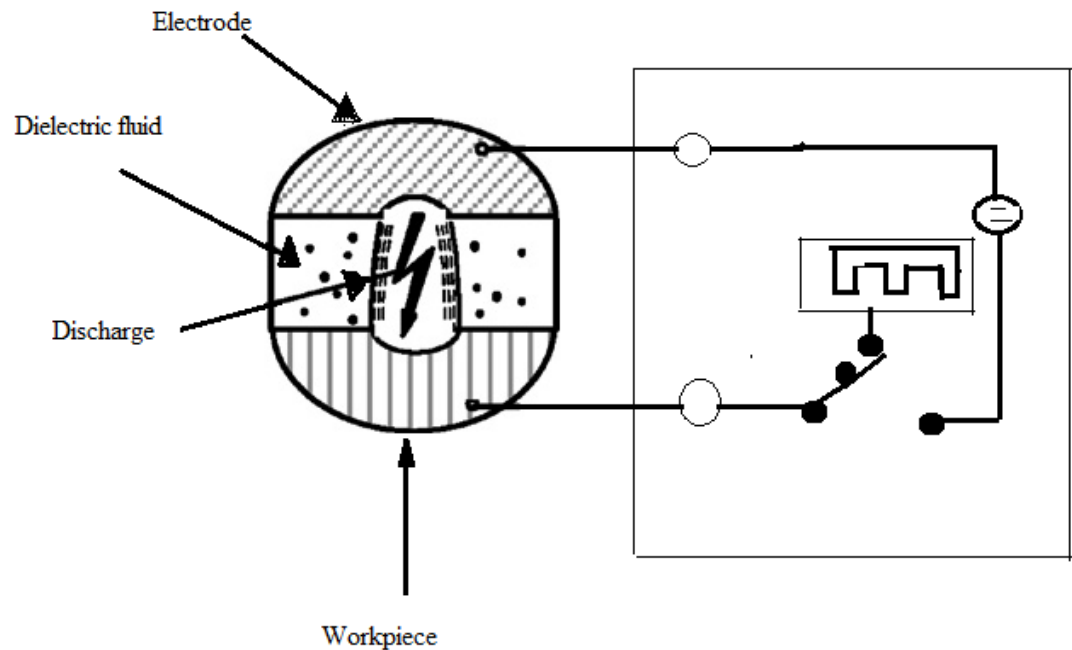


Fig 3: Sparking phenomena in WEDM process

The principle of spark erosion is simple. The workpiece and tool are placed such a way that these don't touch each other. These are separate through a gap which is filling with dielectric fluid. The cutting mechanism therefore takes place in a container. The workpiece and tool are connected to a direct current source. There is a switch in one lead. When this is closed, an electrical potential is applied between the workpiece and tool. At initially no current flows since the dielectric between the workpiece and tool is an insulator. If gap is decreases then a spark jumps across it when it reaches a certain very small size. In this process, current is converted into heat and form plasma channel. Surface of the materials is very powerfully heated in the area of

the discharge channel. If the flow of current is sporadic the discharge channel collapses very quickly. Therefore the molten metal on the surface of the material evaporated explosively and takes liquid material with it down to a certain depth. A small crater is formed. If one discharge is followed by another, new craters are formed next to the previous ones and the workpiece surface is constantly eroded.

1.1.3 Terms used in WEDM process

- **Spark Gap**

Space between electrode and workpiece is called spark gap. Here voltage is applied. The electric field created throughout the space between these electrodes.

- **Kerf width**

It is the sum of the wire diameter and twice of spark gap. The kerf width is generally measured using the Infinite Focus Alicona Machine.

1.1.4 The use of Dielectric in WEDM Process

- **Insulation**

One significant purpose of the dielectric is to insulate the workpiece from the electrode.

- **Cooling**

Due to high temperature, overheating of the electrode and wear can generate. So to avoid this wear, dielectric must cool both the electrode and workpiece.

- **Removal of waste particles**

Particles which are created during the machining must be removed from the area of erosion by the dielectric to avoid disruptions in the process.

1.1.5 WEDM applications in industry

- Dies and punches for Electronic and hierological components.
- Micro surgical tools and biomedical devices.
- Precision flexures for micro positioning systems.
- Miniature spool valves.
- Thin walled structural parts for aerospace industries.
- Precision form gauges for different profiles
- WEDM developments

1.2 Objective of the Present Work

- To determine the temperature distribution, displacement and stress distribution in wire electrode tool of WEDM using FEM analysis.
- To develop a thermo-structural modeling of wire electrode tool for analyzing the effect of built-in temperature to the machining performance.

Chapter 2

- Literature Review

[Kunieda and Furudate \[2\]](#) defined the development of a new dry wire electrical discharge machining method. They were conducted an experiment without using dielectric liquid, instead of dielectric liquid they used only gas atmosphere. For improving the accuracy of finish cutting, the vibration of the wire electrode is required to be minimizing with the negligibly small process reaction force. High accuracy and finish cutting may be recognized in dry-wire electrical discharge machining. But, some disadvantages of dry wire electrical discharge machining like lower material removal rate comparison to conventional wire electrical discharge machining and lines are more likely to be generated over the finish surface.

[Okada et al. \[3\]](#) introduced a fine wire electrical discharge machining using thin wire electrode. In wire electrical discharge machining process, uniform distribution of spark location is essential to achieved for stable machining performance. But, it is difficult to precisely evaluate the distribution of spark location by the conventional branched electric current method when workpiece is considered as thin. Hence, they proposed a new method to analyze the distribution of spark location using a high-speed video camera. From this camera, locations of sparks are identified and analyzed through the recorded images. The machining parameters such as servo voltage, pulse interval time and wire running speed are significantly effects on the distribution of spark location.

[Cabanesa et al. \[4\]](#) introduced a methodology which facilitated to avoid wire breakage and unstable situations as both phenomena reduce process performance and can cause low quality components in wire electrical discharge machining. The proposed methodology establishes the procedures to follow in order to understand the causes of wire breakage and instability. In order to quantify the trend to instability of a given machining situation, a set of indicators in relation to discharge energy, ignition delay time, and peak current has been defined. Wire breakage risk

associated to each situation was evaluated comparing the evolution of those indicators with some previously defined threshold values. The result obtained will be used to develop a real-time control strategy for increasing the performance of the WEDM process.

[Saha et al. \[5\]](#) developed a simple FE model and a new method to predict the thermal distribution in the wire equally and precisely. The model can be used to optimize the different parameters of the system to avoid wire breakage. At any instantaneous of time, the spatial heat distribution profile of the wire can be mapped on the transient analysis of any point on the wire traversing through all the heat zones from the top spool to the bottom end. Based on this principle, the finite element model and optimization algorithm were used to determine the heat generated that mainly responsible for wire breakage. The model successfully predicted the thermal distribution profile accurately for various wire materials, for increased wire velocity and for reduction in heat transfer coefficient. This simple model was a precursor of development for 3-D finite element models which can be described the cross-sectional wire erosion as the workpiece cutting progresses. The modeling may lead to the development of a smart electro-discharge machining system with a sensor and feedback control to increase the cutting speed and minimize breakage.

[Hou et al. \[6\]](#) developed the double layer structure model that analyzed the effect of temperature field and thermal stress on material removal of insulating ceramics Si₃N₄ during the wire electrical discharge machining (WEDM) process. The distributions of temperature filed in conductive layer and Si₃N₄ and double layer structure model during single electrical discharge were compared. And the influences of peak current, pulse duration and the movement speed of wire electrode to discharge craters were researched. The simulation shows that the conductive layer on insulating ceramics makes a larger effect on thermal transmission in the radius direction of discharge crater when discharge occurs. The simulation for temperature field tells that, with

the boiling removal form hypothesis, the material removal volume during single discharge is increasing with the increment of peak current and pulse duration but decreasing with the raising of wire electrode movement speed.

[Hada and Kunieda \[7\]](#) investigated the optimum machining conditions in wire electrical discharge machining (wire-EDM). Discharge current was influenced by the impedances of the wire and workpiece electrodes which may vary depending on the diameter of the wire, height of the workpiece and materials of wire and workpiece even if the pulse conditions are the same. Hence, they developed a simulator to analyze the distribution of the current density, and magnetic flux density in and around the wire to obtain the impedances of the wire and workpiece electrodes using the electromagnetic field analysis by finite element method (FEM). The impedances measured using an LCR meter coincided with the analysis results. Thus it was confirmed that this analysis is useful to obtain the discharge current waveform which may change depending on the dimensions and material properties of the electrodes, serving a tool to optimize the machining conditions.

[Cabanès et al. \[8\]](#) discusses the results of the analyses of an exhaustive experimental database that reproduces unexpected disturbances that may appear during normal operation. The results of the analyses reveal new symptoms that allow one to predict wire breakage. These symptoms are especially related to the occurrence of an increase in discharge energy, peak current, as well as increases and/or decreases in ignition delay time. The differences observed in the symptoms related to workpiece thickness are also studied. Another contribution of this paper is the analyses of the distribution of the anticipation time for different validation tests. Based on the results of the analyses, this paper contributes to improve the process performance through a novel wire breakage monitoring and diagnosing system. It consists of two well differentiated parts: the

virtual instrumentation system (VIS) that measures relevant magnitudes, and the diagnostic system (DS) that detects low quality cutting regimes and predicts wire breakage. It has been successfully validated through a considerable number of experimental tests performed on an industrial WEDM machine for different workpiece thickness. The efficiency of the supervision system has been quantified through an efficiency rate.

Cheng et al. [9] determined a method of the convective heat transfer coefficient in wire electro-discharge machining (WEDM) is introduced. A special device is developed to measure the average temperature increment of the wire after a period of short circuit discharges, and the thermal load imposed on the wire is also tracked and recorded in advance. Then, based on the thermal model of the wire, the convective coefficient can be calculated accurately. Some tuning experiments are carried out inside and outside a previously cut profile to examine the influence of the kerf on the convective coefficient. As soon as the wire cuts into the workpiece, the convective coefficient will decrease more than 30%. With this method, the effect of the coolant flushing pressure on the convective coefficient is also estimated. If the pressure is raised from 0.1 to 0.8 Mpa, the convective coefficient will increase more than 20%, and thus ameliorate the cooling condition of the WEDM process

Yan and Lai [10] presented the development and application of a new fine-finish power supply in wire-EDM. The transistor-controlled power supply composed of a full-bridge circuit, two snubber circuits and a pulse control circuit was designed to provide the functions of anti-electrolysis, high frequency and very-low-energy pulse control. Test results indicated that the pulse duration of discharge current can be shortened through the adjustment of capacitance in parallel with the sparking gap. High value of capacitance contributes to longer discharge duration. A high current-limiting resistance results in the decrease of discharge current. Peak

current increases with the increase of pulse on-time and thus contributes to an increase in thickness of recast layer. Experimental results not only verify the usefulness of the developed fine-finish power supply in eliminating titanium's bluing and rusting effect and reducing micro-cracking in tungsten carbide caused by electrolysis and oxidation, but also demonstrate that the developed system can achieve a fine surface finish as low as $0.22 \mu\text{m Ra}$.

Yuan et al.[11] discussed about the development of reliable multi-objective optimization based on Gaussian process regression (GPR) to optimize the high-speed wire-cut electrical discharge machining (WEDM-HS) process, considering mean current, on-time and off-time as input features and material remove rate (MRR) and Surface Roughness (SR) as output responses. In order to achieve an accurate estimation for the nonlinear electrical discharging and thermal erosion process, the multiple GPR models due to its simplicity and flexibility identify WEDM-HS process with measurement noise. Objective functions of predictive reliability multi-objectives optimization are built by probabilistic variance of predictive response used as empirical reliability measurement and responses of GPR models. Finally, the cluster class centers of Pareto front are the optional solutions to be chosen. Experiments on WEDM-HS (DK7732C2) are conducted to evaluate the proposed intelligent approach in terms of optimization process accuracy and reliability. The experimental result shows that GPR models have the advantage over other regressive models in terms of model accuracy and feature scaling and probabilistic variance. Given the coefficient parameters, the experimental optimization and optional solutions show the effectiveness of controlling optimization process to acquire more reliable optimum predictive solutions.

Fuzhu et al. [12] discussed about the coupled thermo-mechanical analysis, both the three-dimensional temperature and also the stress distributions in the micro wire are determined. As a

result, the tension of the micro wire electrode during the WEDM process can be optimized in accordance with the discharge energy, which is sampled and fed back to the tension control system in real time. Then the development of an optimal tension control system characterized by the form of master-slaver structure makes it possible to keep the wire tension optimal in the process of WEDM. The results of the machining experiments show that the optimal wire tension control is effective on the improvement of the machining accuracy with the prevention of wire breakage for the micro WEDM.

[Sanchez et al. \[13\]](#) introduced a new approach to the prediction of angular error in wire-EDM taper-cutting is presented. A systematic analysis of the influence of process parameters on angular error is carried out using Design of Experiments (DoE) techniques. A quadratic equation for the prediction of angular error that takes into account electrical parameters and part geometry is derived. Validation results reveal a dominant influence of the mechanical behaviour of then wire, rather than that of EDM regime. Following this assertion an original finite element model (FEM) to describe the mechanical behaviour of soft wires, typically used in taper-cutting operations, has been developed taking into account non-linear phenomena such as contact mechanics, plastic behaviour, stress-stiffening and large displacements. Both the results of DoE techniques and FEM simulation have been validated through experimental tests in industrial conditions.

[Shichun et al. \[13\]](#) introduced the kerf variations in micro-WEDM, and the mathematical model of wire lateral vibration in machining process is established and its analytical solution is obtained. The model is practically verified on a self-developed micro WEDM machine. Under this model, a 30.8 μm width slot is achieved on a stainless steel work-piece with $\text{Ø}30$ mm wire-tool.

Liao and Yu [14] introduced the relationship between machining parameters and machining characteristics of different materials in WEDM. It is difficult to obtain because a large number of experiments must be conducted repeatedly. A new concept attempting to solve this problem is presented in this paper. The specific discharge energy (SDE) defining as the real energy required to removing a unit volume of material is proposed. The SDE is constant for a specific material. Experimental results reveal that the relative relationship of SDE between different materials is invariant as long as all materials are machined under the same machining conditions. It is also found that the materials having close value of SDE demonstrate very similar machining characteristics such as machining speed, discharge frequency, groove width and finish of the machined surface under the same machining conditions. The result obtained can be applied for the determination of the settings of machining parameters of different materials.

Takayuki et al. [15] introduced the arbitrary shape machining method of Si₃N₄ insulating ceramics by WEDM. In the WEDM of thick work-pieces of Si₃N₄ insulating ceramics, wire breakages occurred frequently. To avoid the breakage conditions, a new assisting electrode material was used. Using this method, a thin ceramics sheet was hollowed out of Si₃N₄ ceramics without breakages. In the machining of thin sheets, a warping phenomenon is observed to occur towards the end of the product owing to thermal residual stress. The amount of warp is dependent on, and can be reduced considering, the machining path. Furthermore, the axisymmetric products can be machined by this method with a rotating work-piece system.

Albert and Su [16] introduced the tapering process of WEDM, which can generate curved surfaces on workpiece, is a very unique ability of this machining process. This report is dedicated to the removal analysis of tapering WEDM and to the improvement of contouring accuracy in application to conjugate surfaces. An inclined discharge angle (IDA) analysis was

proposed to study the removal mechanism with a novel point of view. Based upon the analysis, a theoretical removal model was proposed. Furthermore, it might be reasonable that the machining load and contouring error could be inferred from the removal burden. Therefore, an improvement strategy including control of discharged power and wire tension was proposed to adapt to the variation of machining load. Effects of the proposed method were verified through experiments. It is evident that the tapering accuracy was improved significantly, and it is feasible to the generation of precise conjugate surface.

[Alias et al. \[17\]](#) stated that improper electrical parameters settings can affect the processing efficiency and surface roughness due to arcing phenomenon that lead by discharge point of focus. Objective of the paper is to uncover the influence of three different machine rates which are 2 mm/min, 4 mm/min and 6 mm/min with constant current (6A) with WEDM of Titanium Ti-6Al-4V. The effects of different process parameters on the kerf width, material removal rate, surface roughness and surface topography are also discussed. The best combination of machining parameter viz. machine feed rate (4 mm/min), wire speed (8 m/min), wire tension (1.4kg) and voltage (60V) were identified. The paper highlights the importance of process parameters and different machining conditions on kerf width, MRR, surface roughness (Ra) and surface topography.

[Dodun et al. \[19\]](#) conducted an electrical discharge machining process between a travelling wire tool electrode and a plate workpiece for detach parts characterized by machined ruler surfaces. The practical experience and the study of the specialty literature highlighted the possibilities to improve the material removal rate by acting on the wire tool electrode two versions of devices able to periodically change the wire traveling motion speed are discussed and proposed. The

devices could be included in the circuit of guiding the wire electrode on the wire electrical discharge machine.

Chapter 3

Modelling of WEDM

- Modeling procedure using ANSYS
- Process of Thermal Modeling using ANSYS software
- Process of structural Modeling using ANSYS software
- Process of Thermo-structure Modeling using ANSYS software

3 Modelling procedure using ANSYS of WEDM

In the wire EDM, a series of rapid electric spark occur in the gap between tool (wire) and workpiece. Addition of particles into the dielectric fluid makes this process more complex and random. The following assumptions are made without sacrificing the basic features of the wire EDM model to make the problem mathematically feasible.

3.1 Thermal model of Wire EDM

The working principal of WEDM is as same EDM process, when the distance between the two electrodes (wire and the workpiece) is reduced the intensity of electric field in the volume between the electrodes (wire and the workpiece), become greater than the strength of the dielectric, which breaks, allowing current to flow between the two electrodes. For this reason the spark will generated.

3.1.1 Assumption

The mathematical statement that describes the temperature variation along the wire axis in the wire-EDM process is formulated under the following:

Assumptions:

- The model is developed for a single spark.
- The thermal properties of workpiece material are considered as a function of temperature. It is assumed that due to thermal expansion, density and element shape are not affected.
- Temperature analysis is considered to be of transient type.
- The material of the wire is homogeneous, isotropic and has constant properties.

- The heat source is assumed to have Gaussian distribution of heat flux on the surface of the workpiece.
- The composition of the material of workpiece is assumed to be homogeneous and isotropic.

3.1.2 Thermal Model

The discharge phenomenon in wire EDM can be modeled as the heating of the work piece by the incident plasma channel. The mode of heat transfer in solid is conduction.

3.1.3 Governing equation

This is the equation for calculation of transient temperature distribution with in workpiece. The differential governing equation of thermal diffusion differential equation in a model is governed by the following.

$$\frac{\partial}{\partial r} \left(k_w \frac{\partial T}{\partial r} \right) + \frac{1}{r^2} \frac{\partial}{\partial \theta} \left(k_w \frac{\partial T}{\partial \theta} \right) + \frac{\partial}{\partial z} \left(k_w \frac{\partial T}{\partial z} \right) + q''' = \rho c \frac{\partial T}{\partial t} \quad (1)$$

Where r and θ are the radial and angle coordinates respectively, z is the axial coordinate, ρ and c are the density and the specific heat of the wire material, k_w thermal conductivity of the wire material and T is the temperature of the micro element in the wire.

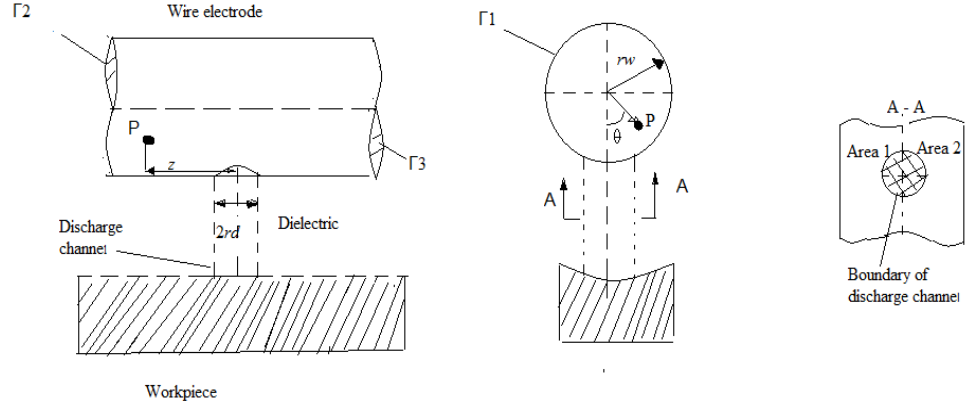


Fig. 4 Three-dimensional thermal analysis model for WEDM [12]

3.1.4 Boundary conditions

The boundary between area1 and area 2 can be mathematically determined by the following equations:

$$\mathbf{r} = \mathbf{r}_w \quad (2)$$

$$(\mathbf{r}_w \sin \theta)^2 + \mathbf{z}^2 = \mathbf{r}_d^2 \quad (3)$$

Where r_d is defined as the radius of the discharge channel, r_w is the wire radius, and Γ_1 represents the cylindrical boundary between the wire and the dielectric.

From fig. 4: in inside area 2, the thermal equilibrium can be described as the following equations:

$$\mathbf{If} \ \mathbf{r} = \mathbf{r}_w \ \text{and} \quad (\mathbf{r}_w \sin \theta)^2 + \mathbf{z}^2 > \mathbf{r}_d^2 \quad (4)$$

$$\text{Then } k_w \frac{\partial T}{\partial r} = h(T - T_0) \quad (5)$$

Where, h is the heat transfer coefficient, T_0 is the initial temperature of wire electrode and T Temperature.

3.1.5 Material properties

In wire EDM process, huge thermal energy is generated, so material properties are required for analysis this process. In this paper two materials are taken:

Brass wire

The chemical composition of brass is 62% Cu and 38% Zn.

Table 1: Properties of brass wire

Properties	Unit	Value
Density	Kg/m ³	8490
Thermal conductivity	W/m-K	115
Specific heat	J / kg-K	380
Modulus of Elasticity	G Pa	97
Bulk Modulus	G Pa	140
Poisson's Ratio		.31
Melting temperature	⁰ C	1083
Shear Modulus	G Pa	37
Solidus	⁰ C	885

Molybdenum wire

Table 2: Properties molybdenum wire

Properties	Unit	Value
Thermal Conductivity	W /m-K	139
Coefficient of linear thermal expansion	K ⁻¹	4.8 x 10 ⁻⁶
Density	kg /m ³	10280
Young's modulus of elasticity	G Pa	329
Poisson's ratio		.31
Shear modulus	G Pa	126
Melting point	⁰ C	2523

3.1.6 Heat Flux due to the wire electrode in a single spark

In this paper, a Gaussian heat distribution is assumed. If it is assumed that total power of power of each pulse is to be used only single spark can be written as follows:

$$q(r) = \frac{k}{\pi R^2(t)} PVI \exp. \left(-\frac{kr^2}{R^2(t)}\right) \quad (6)$$

Where $q(r)$ is the heat flux at the radius of r , k is the heat concentration coefficient ($k=4.5$, Kunieda et al. case), $R(t)$ is the radius of arc plasma at the moment of t , P is the energy distribution coefficient ($= 0.38$, Kunieda et al.), V is the voltage between anode and cathode during discharge occur, I is the peak current and r is the distance from the center of arc plasma.

3.1.7 Spark Radius

Spark radius is an important parameter in the thermal modeling of WEDM process. In practice, it is very difficult to measure experimentally, because spark radius very short pulse duration of in microseconds. Ikai and Hashiguch have derived a semi-empirical equation of spark radius

termed as "equivalent heat input radius" which is a function of discharge current, I (A) and discharge on-time, t_{on} (μ s). It is more realistic when compared with the other approaches.

$$\text{Spark radius } (R) = (2.04 e^{-3}) I^{0.43} t_{on}^{0.44} \quad (\mu\text{m}) \quad (7)$$

3.2 Finite Element Analysis Procedure using ANSYS software

3.2.1 Thermal analysis of brass wire

The general finite element modeling procedure consists of the following steps:

i. preferences

- Thermal

ii. Preprocessing

- Definition of Element type
- Material properties definition
- Model generation
- meshing

iii. Solution

- Defining initial condition
- Applying boundary condition
- Applying load
- Solving for results

iv. Post processing

- Reading result file
- Viewing results

3.2.2 Process of thermo-structural modeling

1. Open Mechanical APDL (ANSYS).
2. Go to File > Change Title and give a new title for the example.
3. Preferences
4. Preprocessing>element type> Add/Edit/Delete
 - Click on add
 - Select thermal solid on the left list and Brick 8 node 70 on right list(i.e. element type)
click on OK
 - CLOSE
 - Material properties>temperature unit>Celsius>ok
 - Material Models>thermal >conductivity>isotropic>ok ,put value>density put
value>specific heat put value>material exit
 - Modeling>create>cylinder>solid cylinder>put the dimensions
 - Meshing>mesh tool> smart size 6>mesh >ok

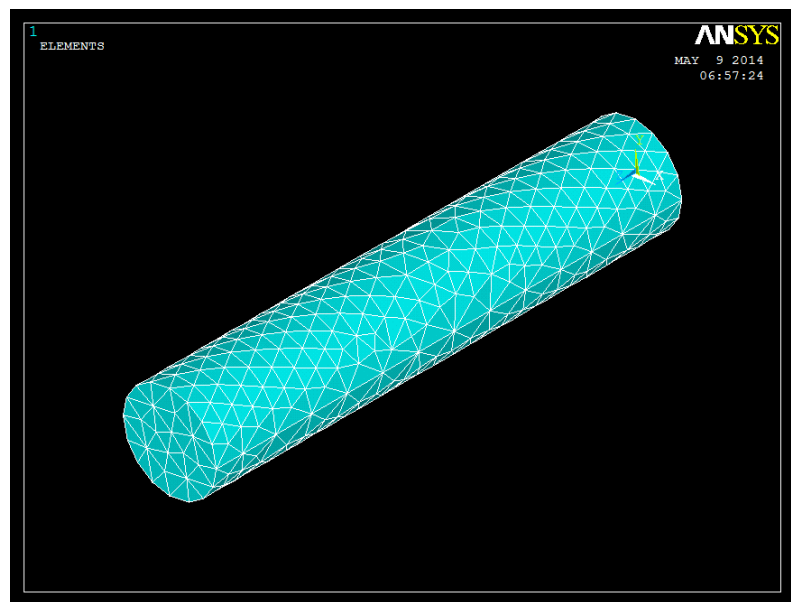


Fig.5: Three-dimensional view of the meshed model

- Physics> Environment>write >physics file title>thermal>ok
- Element type>switch element type>change>element type>thermal to structural>ok
- Material properties>structural>linear>isotropic>thermal expansion>ok>exit
- Physics> Environment>write >erase thermal>write structural>ok
- Solution>new analysis type>transient>full>ok
- Solution control>putting the t_{on} time> Automatic time stepping ON>no. of subsets
- Define loads>apply>functions>read file>ok
- Thermal>heat flux>on element>select proper element>ok
- Initial condition>define>pick all>temperature>21⁰C
- Solve >current LS

5. Post processing>plot results>counter plot>nodal solution>DOF solution>nodal temperature>OK

- Finish
- Physics> Environment>read >structural>ok
- Solution control>putting the t_{on} time> Automatic time stepping ON>no. of subsets
- Apply>structural>displacement>area>all DOF>OK
- Solution load step>write LS file>1>ok
- Analysis type>solution control>basic>off time>transient>ramped loading
- Defineload>apply>temperature>from thermal analysis>browse>file.rth>ok

Post processing>plot results>counter plot>nodal solution>DOF solution>nodal temperature>OK

Chapter 4

Results and Discussions

ANSYS model confirmation

- Thermal modeling of wire EDM for single spark in brass wire
- Thermo-structural analysis of WEDM in brass wire

4.1 ANSYS model confirmation

In this section we have firstly make a model of WEDM process for brass wire with parameter setting as given in Table 3. Later the value has been compared with Han et al. Fig. 6 shows temperature distribution in brass wire, which is approximately same of Han et al. model. So we can say that we are proceeding in right way. Thermal modeling has done in using ANSYS

4.2 FEM analysis

4.2.1 Thermal modeling of wire EDM for single spark in brass wire

Main parameters of the thermal analysis (analysis parameters)

Table 3: Parameters used for thermal analysis in WEDM process

Parameter	Unit	Value
Peak current of electro-discharge	A	27
Voltage of electro discharge,	V	25
Duration of single pulse	μ s	0.12, 0.26, 0.36, 0.52, 0.58, 1.2, 1.82
Wire radius	Mm	0.05
Convective coefficient	$W/m^2 \text{ } ^\circ C$	3040
Temperature of the dielectric	$^\circ C$	21
Poisson' ratio		.31
Coefficient of linear thermal expansion	K^{-1}	1.9×10^{-5}

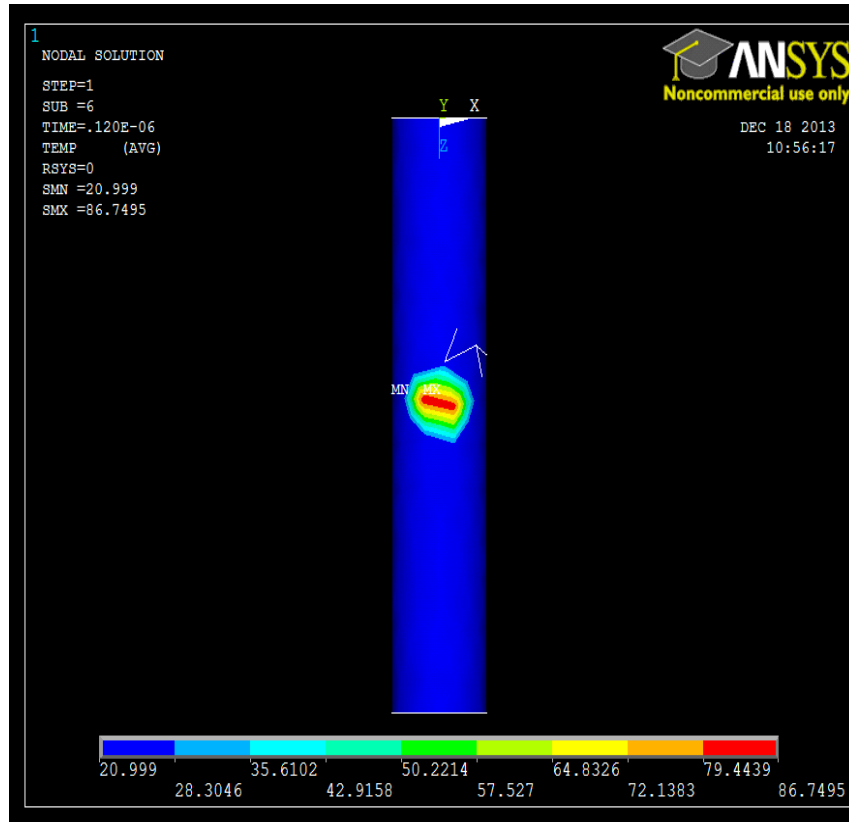


Fig.6: Temperature distribution in Brass wire with $V=25V$, $I=27 A$, $P=0.38$ and $t_{on}=0.12\mu s$

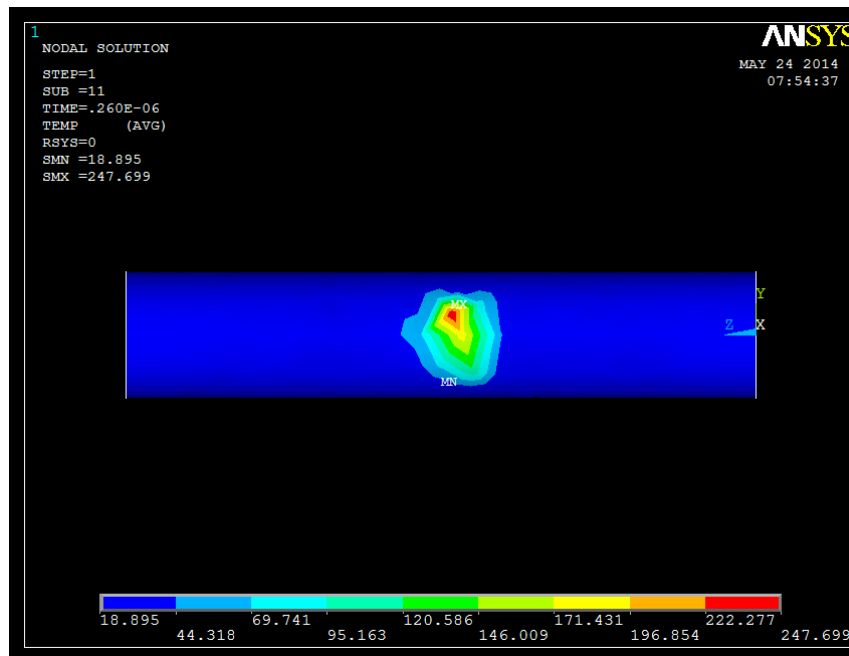


Fig.7: Temperature distribution in Brass wire with $V=25V$, $I=27 A$, $P=0.38$ and $t_{on}=0.26\mu s$

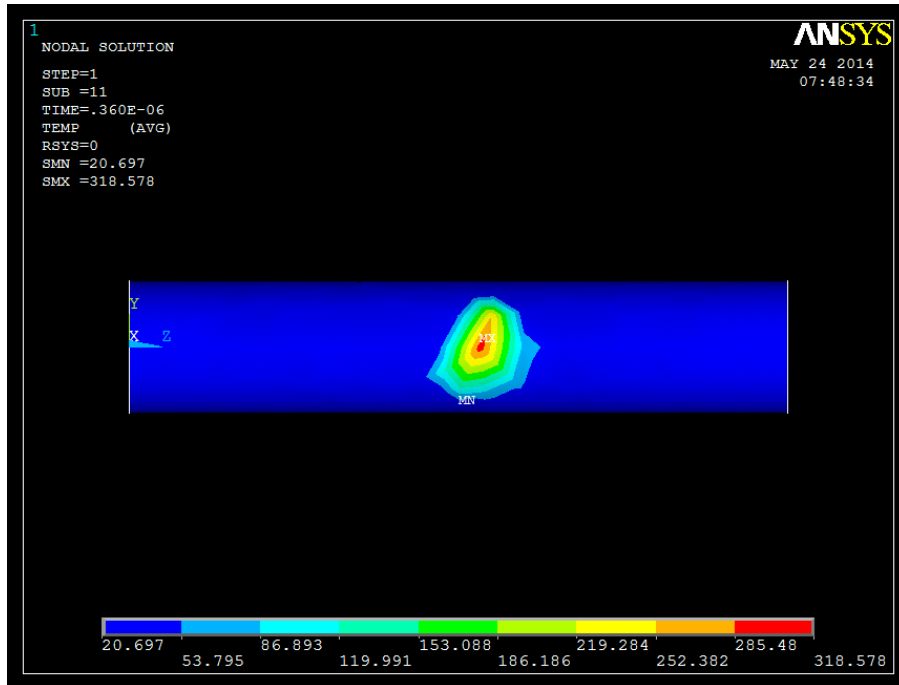


Fig.8: Temperature distribution in Brass wire with $V=25V$, $I=27 A$, $P=0.38$ and $t_{on}=0.36\mu s$

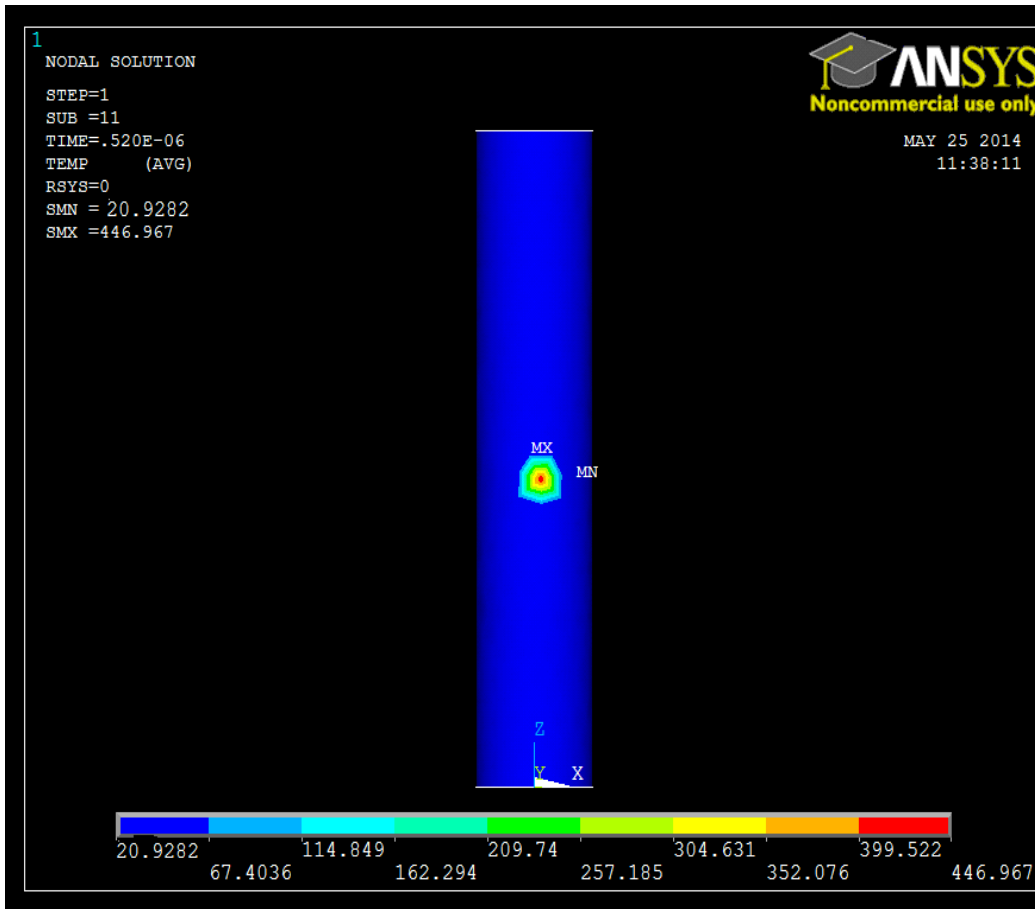


Fig.9: Temperature distribution in Brass wire with $V=25V$, $I=27 A$, $P=0.38$ and $t_{on}=0.52\mu s$

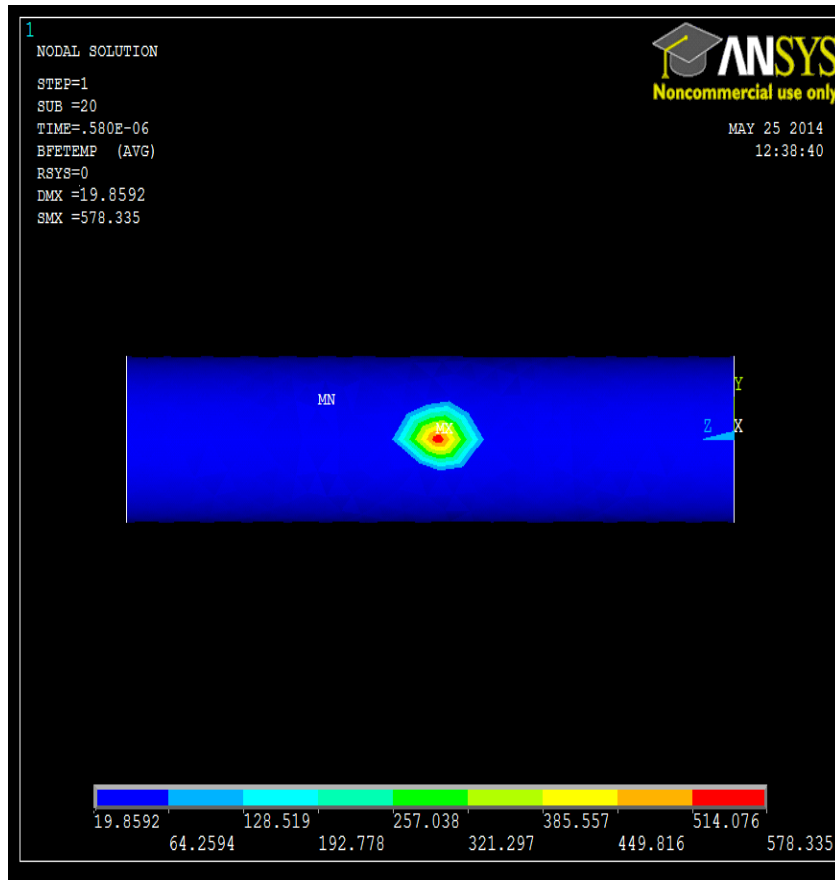


Fig.10: Temperature distribution in Brass wire with $V=25V$, $I=27 A$, $P=0.38$ and $t_{on}=0.58\mu s$

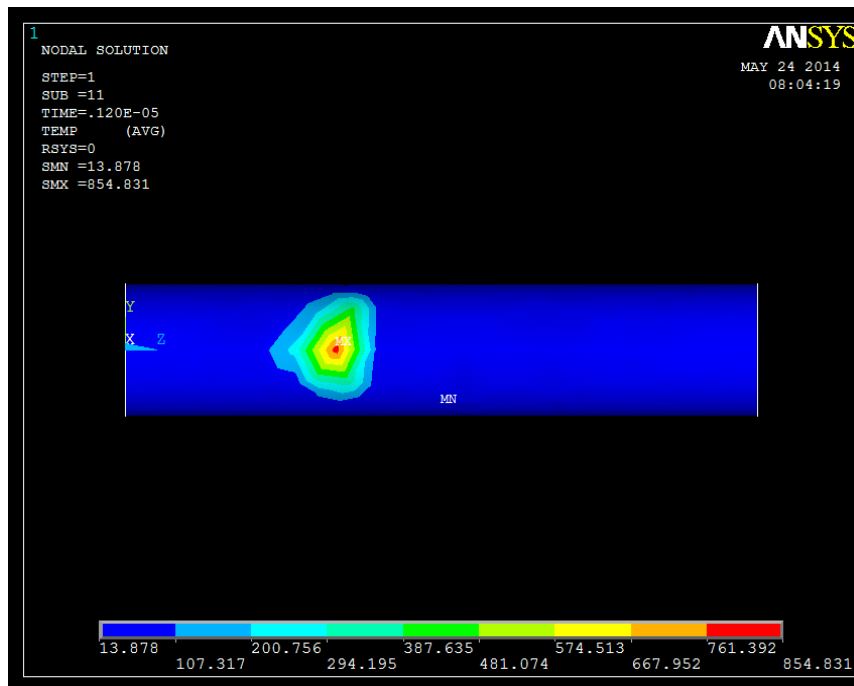


Fig.11: Temperature distribution in Brass wire with $V=25V$, $I=27 A$, $P=0.38$ and $t_{on}=1.2\mu s$

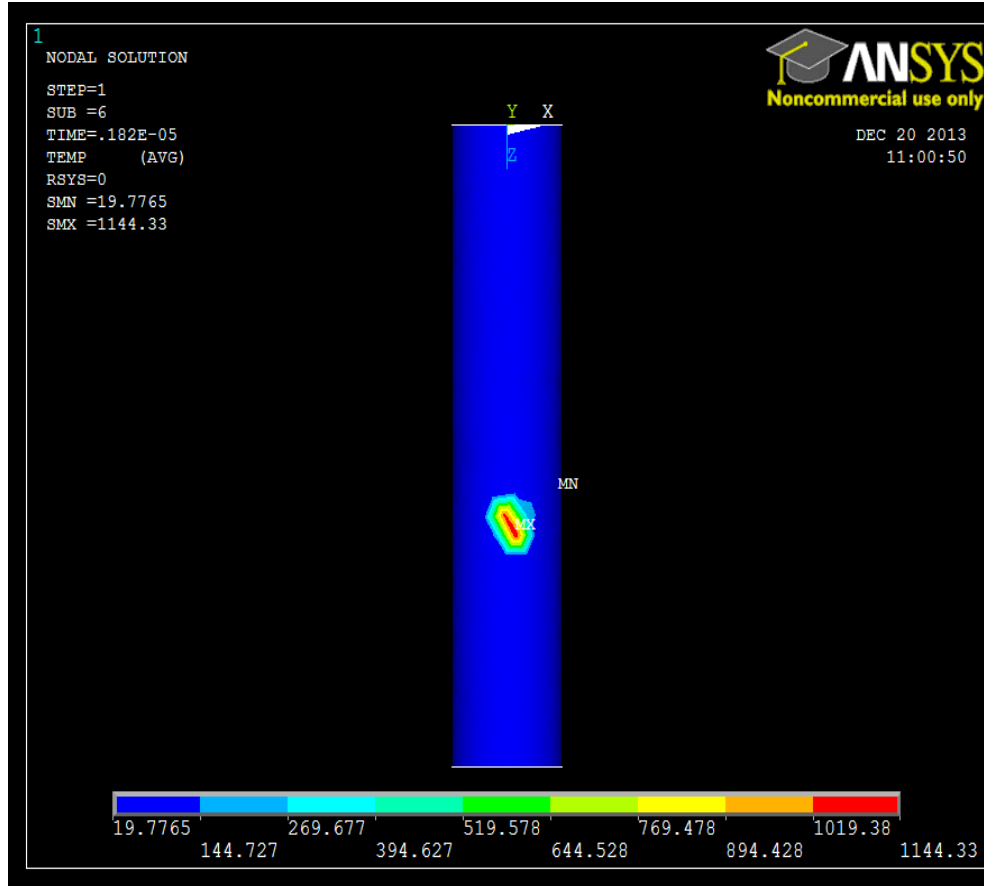


Fig. 12: Temperature distribution in Brass wire with $V=25V$, $I=27 A$, $P=0.38$ and $t_{on}= 1.82\mu s$

4.2.2. Structural modeling of WEDM in molybdenum wire

In this section we have firstly make a model of WEDM process for brass wire with parameter setting as given in Table 4. Later the value has been compared with Saha et al. Fig. 6 shows displacement molybdenum wire, which is approximately same of Saha et al. So we can say that we are proceeding in right way. The structural analysis has done of molybdenum wire.

Displacement analysis in the wire due to tension:

After solving for the temperature distribution we attempt to find the displacement in the wire.

Now in this case molybdenum wire is used. Process parameters used for analysis is shown below

Table 4.

Table 4: Parameters used for structural analysis in WEDM process

Parameter	Units	Value
Radius of wire	Mm	0.125
Length of wire	M	0.1
Tension	N	13.7295
Initial temperature	K	273
Working temperature	K	390

The displacement graph is shown in below:

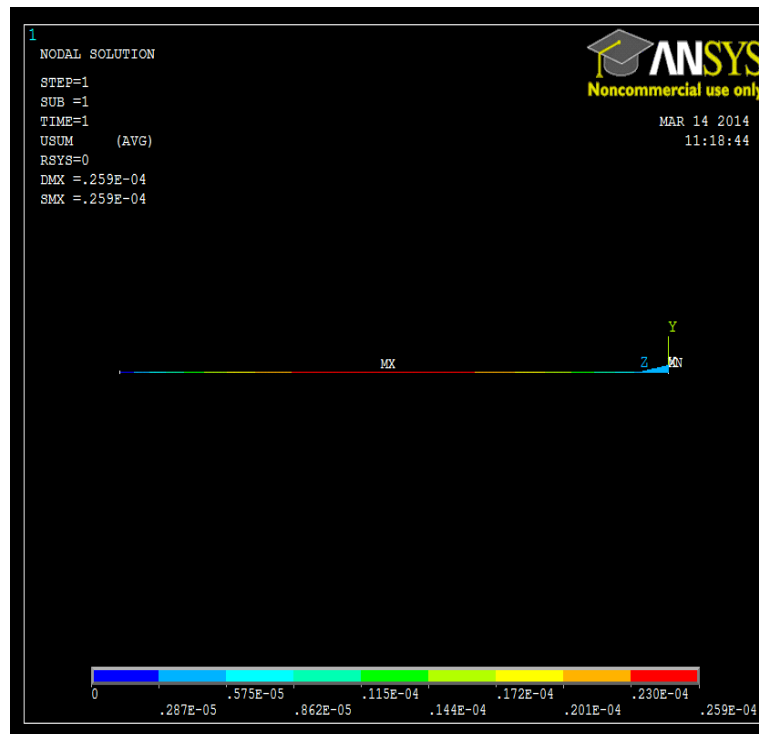


Fig. 13: Nodal solution of displacement

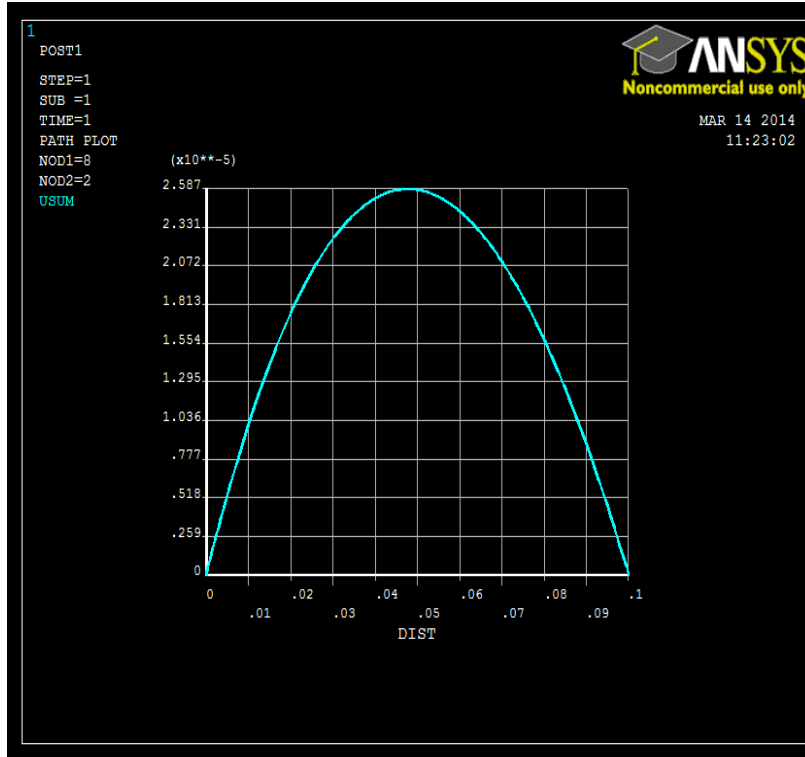


Fig. 14: Graph of displacement

4.2.3. Thermo-structural analysis of WEDM in brass wire.

Thermal stress modelling of micro wire EDM for single discharge

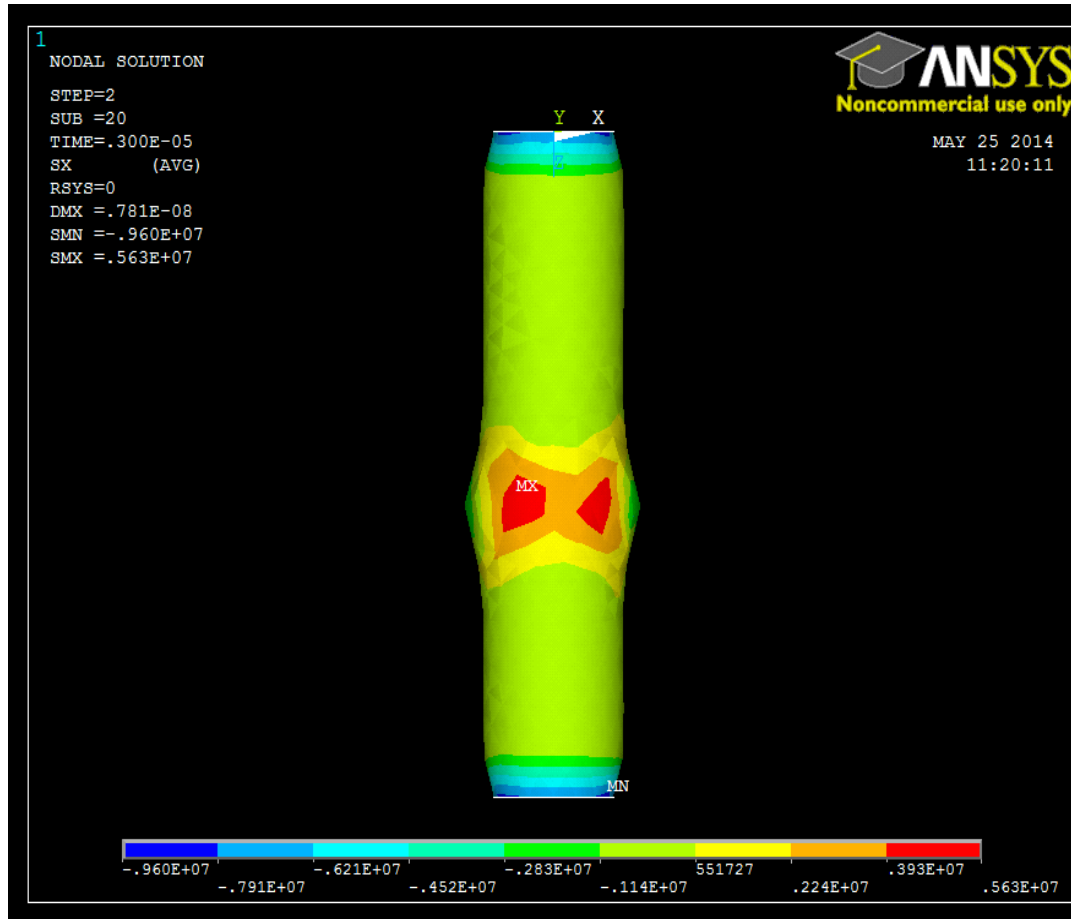


Fig. 15: Thermal Stress in X-component at $t_{on}=0.12\mu s$

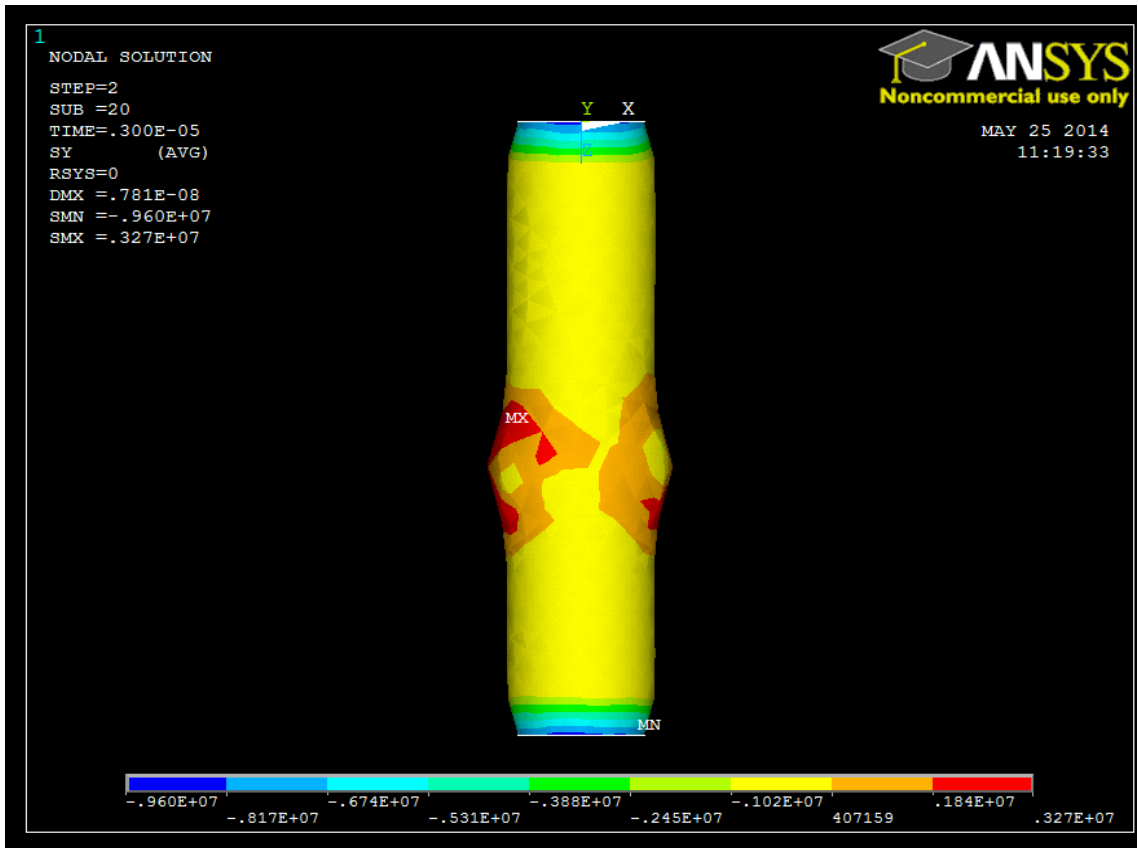


Fig. 16: Thermal Stress in Y-component at $t_{on}=0.12\mu s$

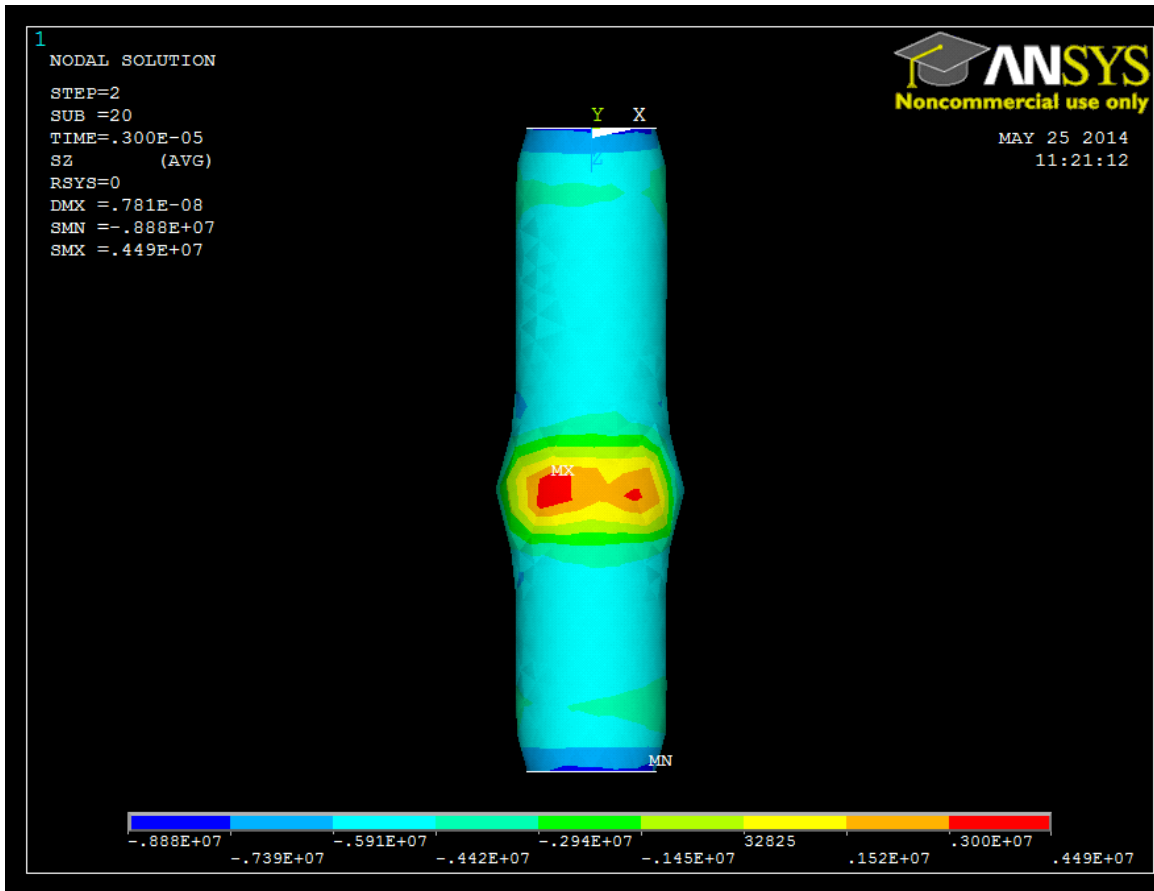


Fig. 17: Thermal Stress in Z-component at $t_{on}=0.12\mu s$

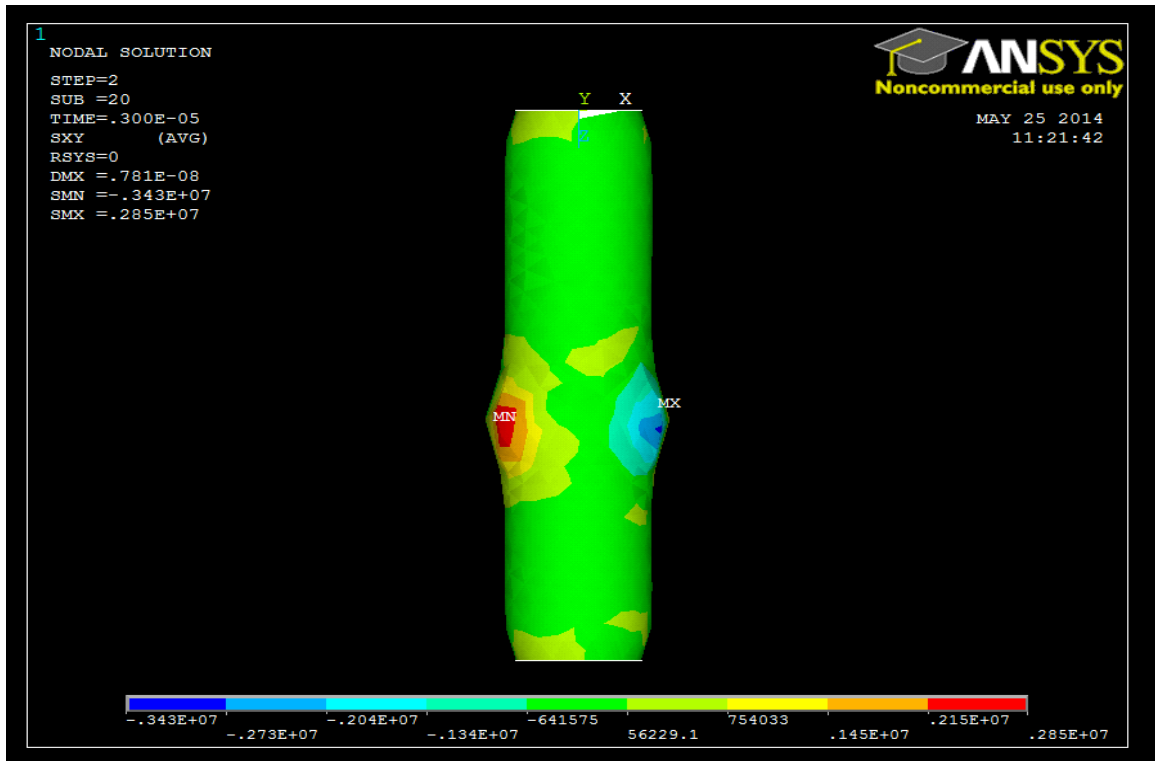


Fig. 18: Thermal shear stress in XY component at $t_{on}=0.12\mu s$

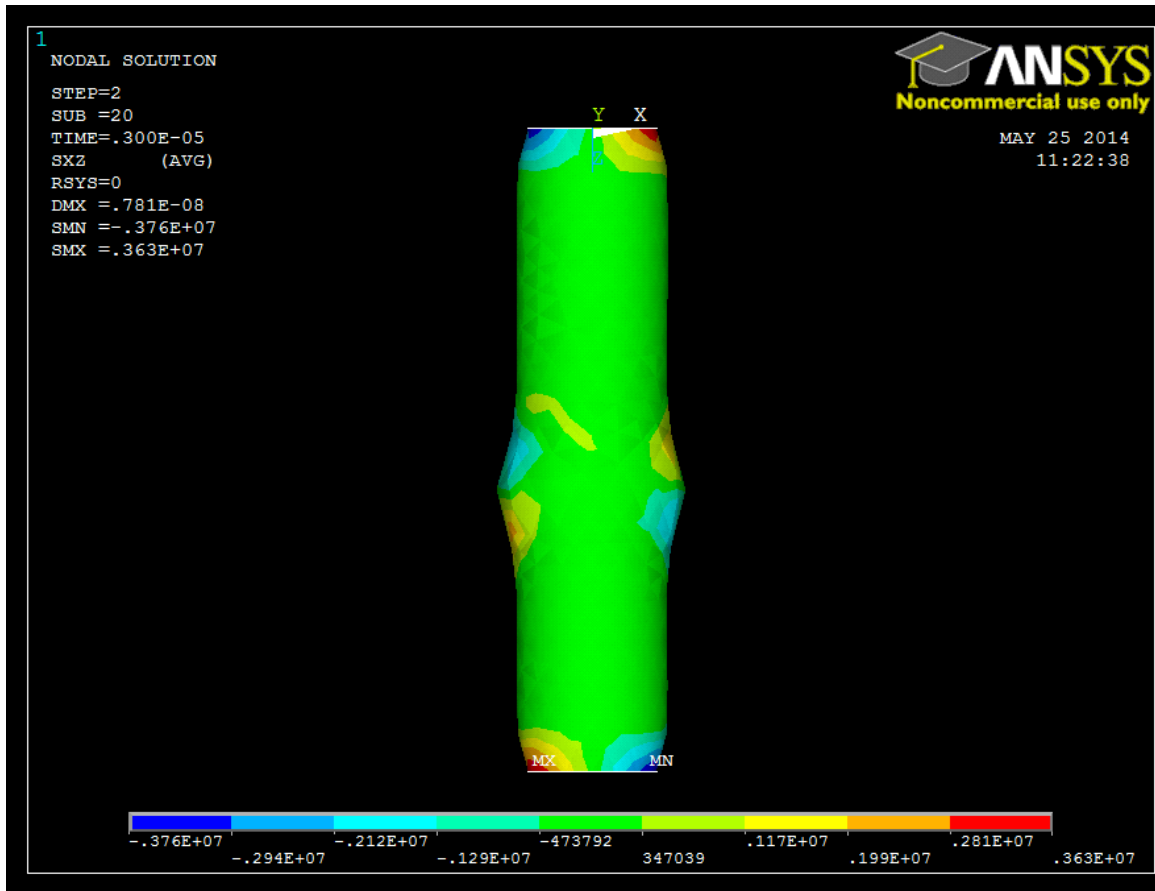


Fig. 19: Thermal shear stress in XZ component at $t_{on}=0.12\mu s$

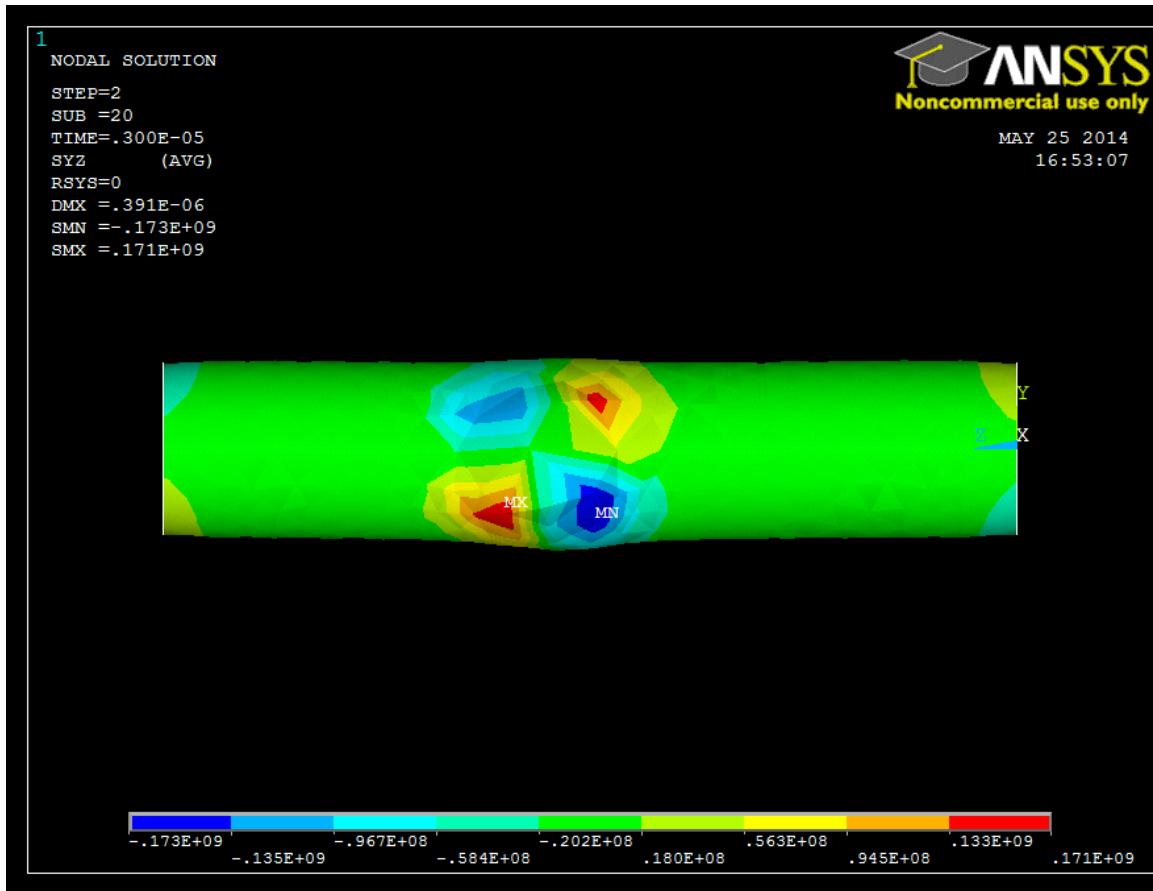


Fig. 20: Thermal shear stress in YZ-component at $t_{on}=0.12\mu s$

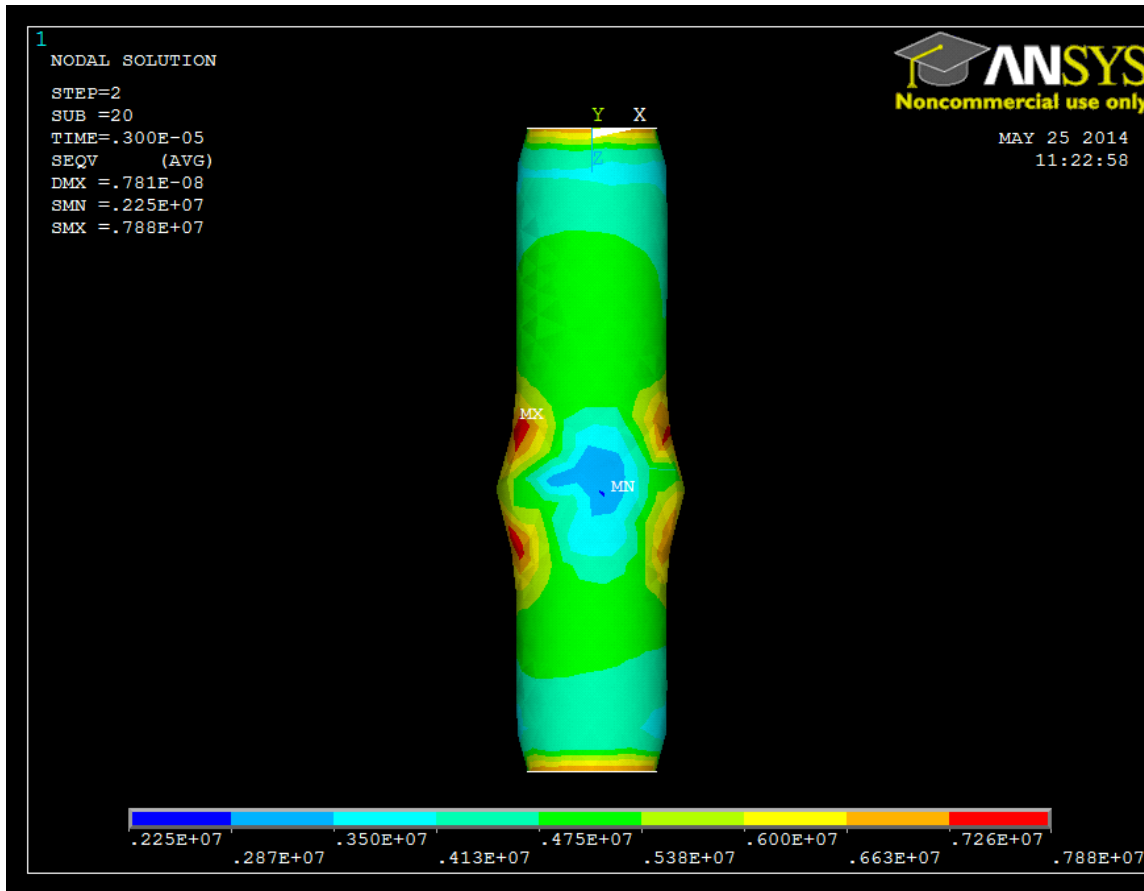


Fig. 21: Residual stress at $t_{\text{off}} = 3\mu\text{s}$

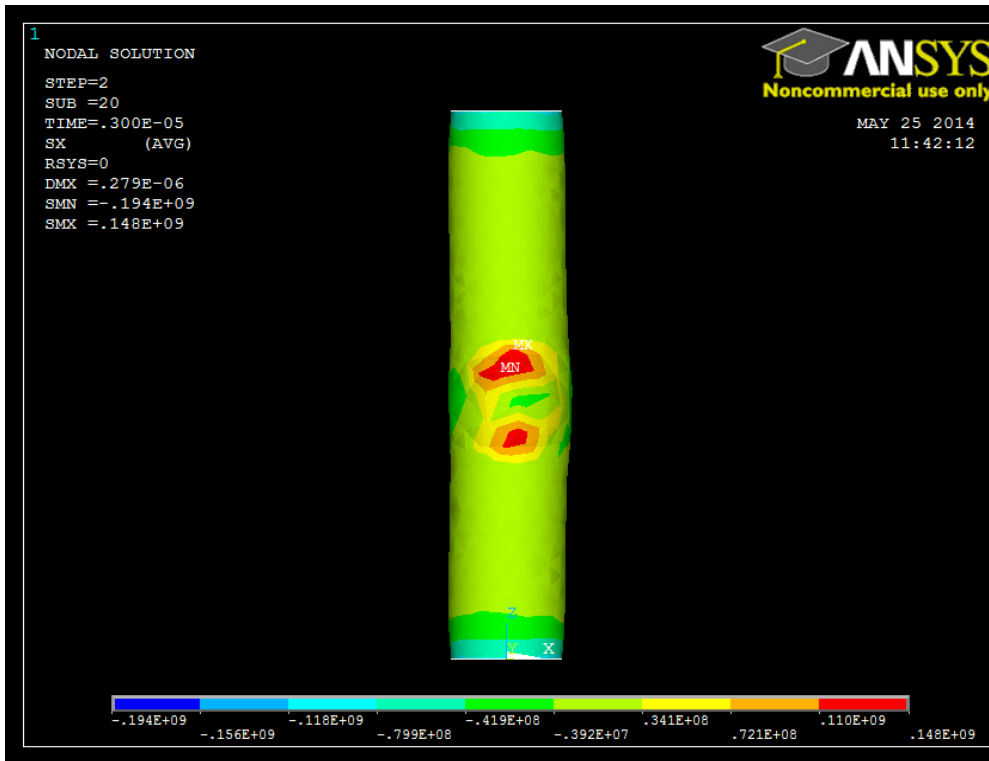


Fig. 22: Thermal Stress in X-component at $t_{on}=0.52\mu s$

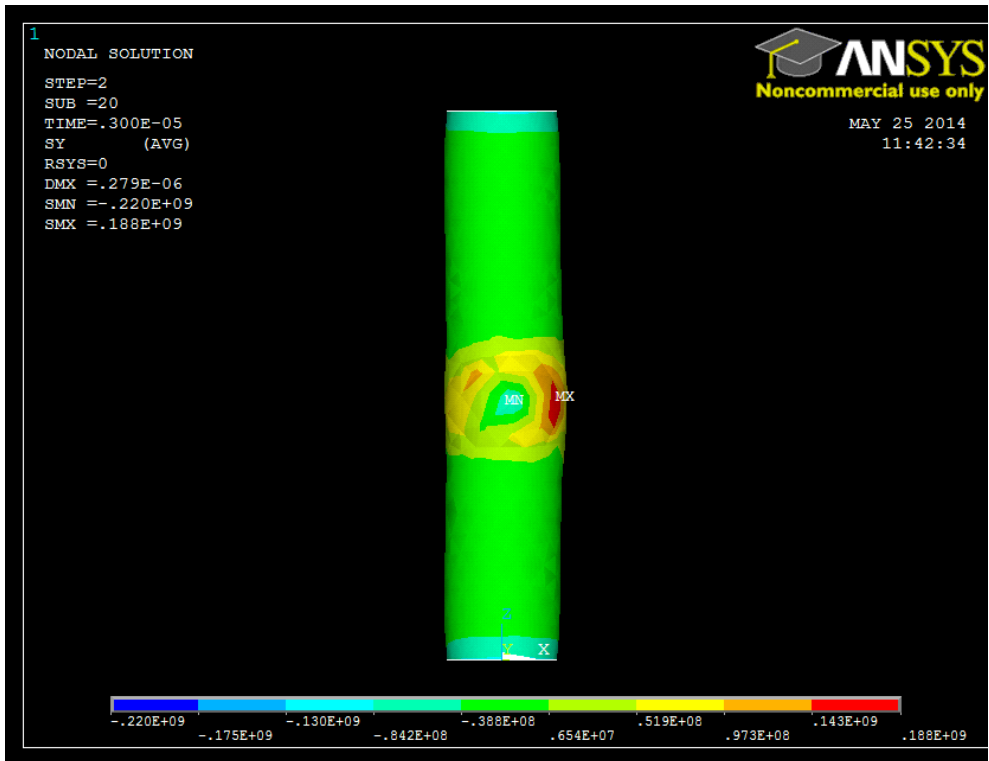


Fig. 23: Thermal Stress in Y-component at $t_{on}=0.52\mu s$

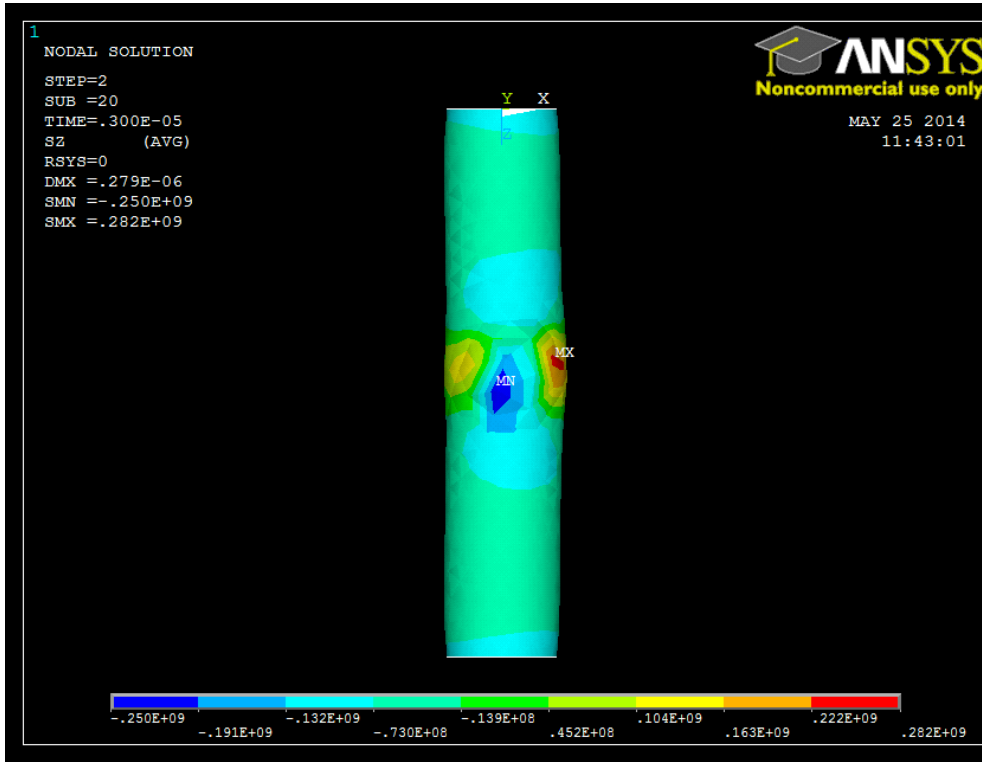


Fig. 24: Thermal Stress in Z-component at $t_{on}=0.52\mu s$

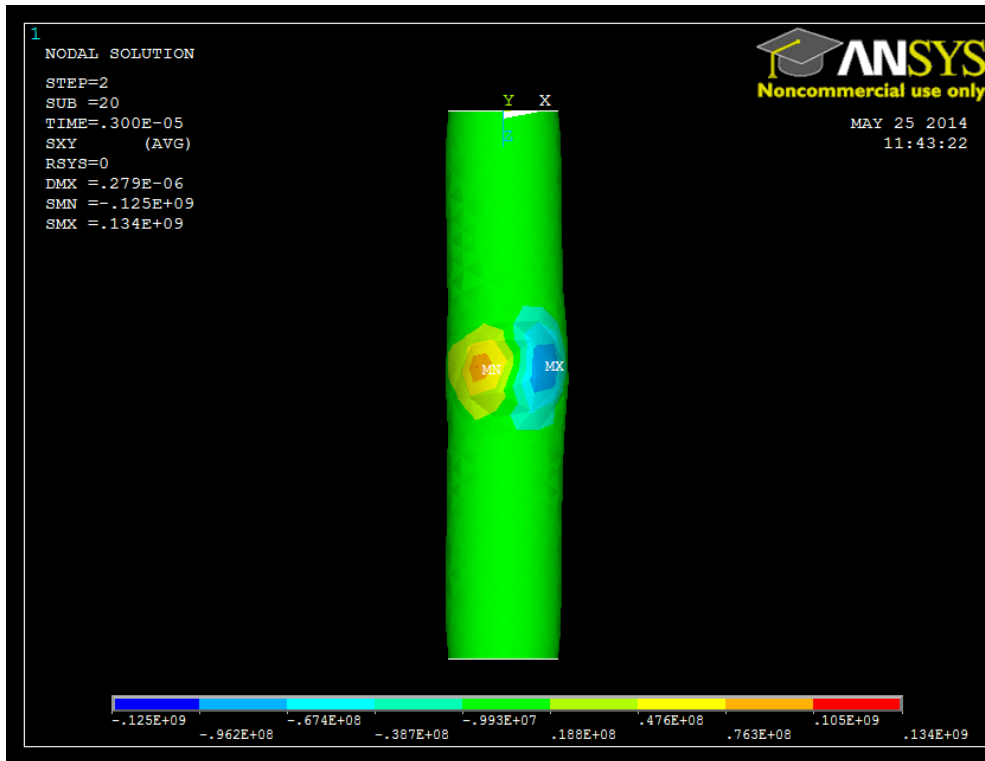


Fig. 25: Thermal shear stress in XY-component at $t_{on}=0.52\mu s$

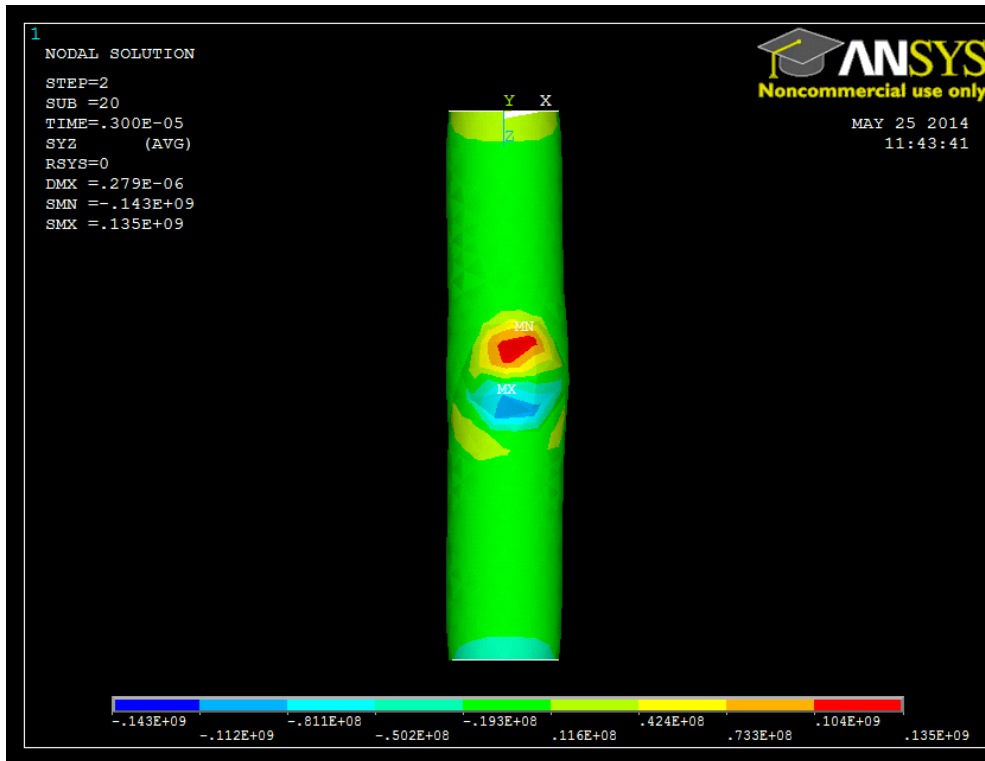


Fig. 26: Thermal shear stress in YZ-component at $t_{on}=0.52\mu s$

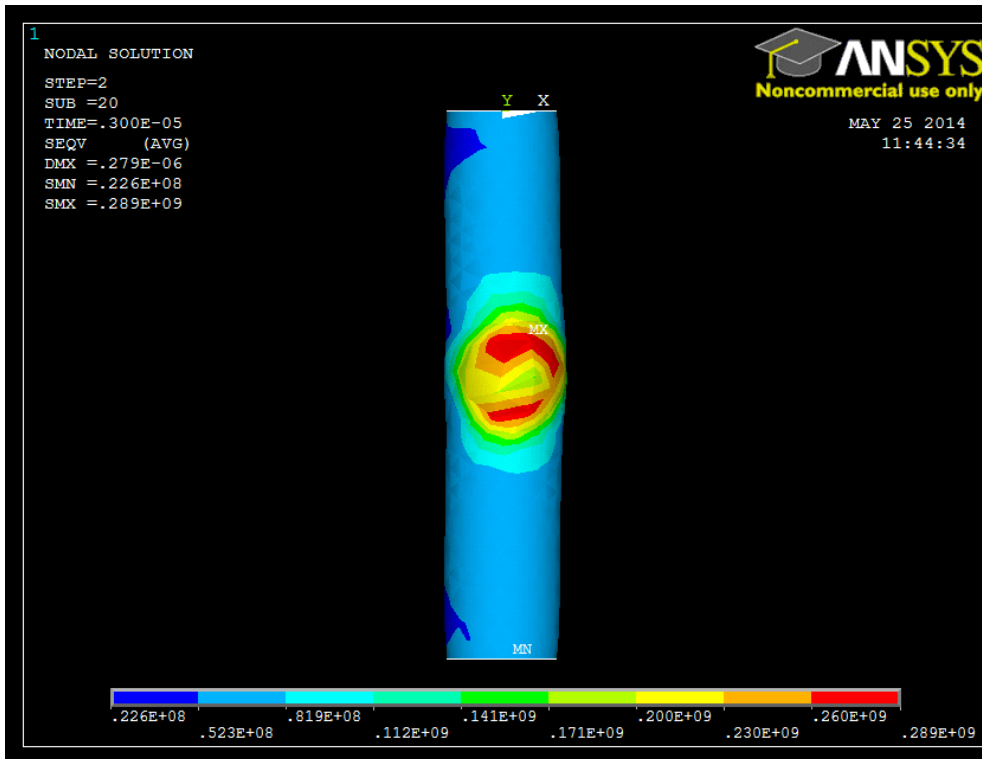


Fig. 27: Residual stress at $t_{\text{off}}= 3\mu\text{s}$

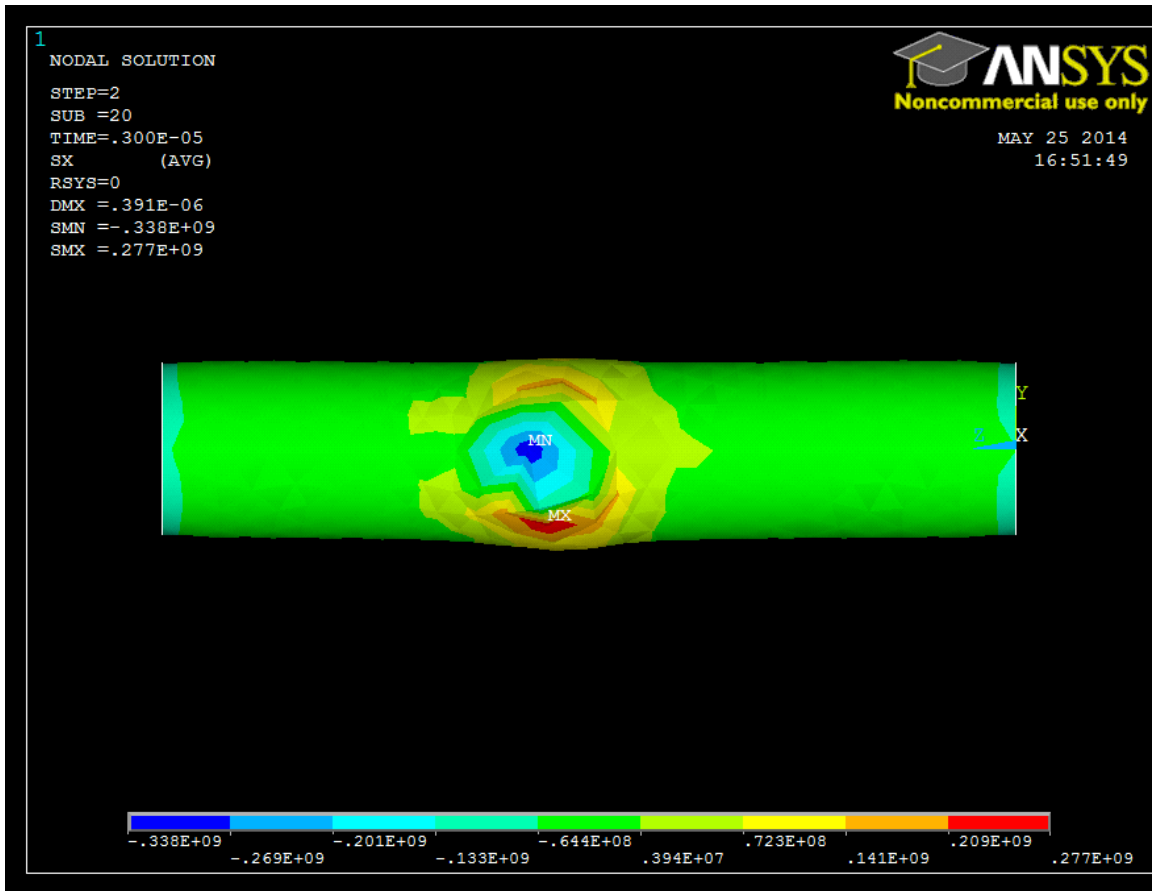


Fig. 28: Thermal Stress in X-component at $t_{on}=1.82\mu s$

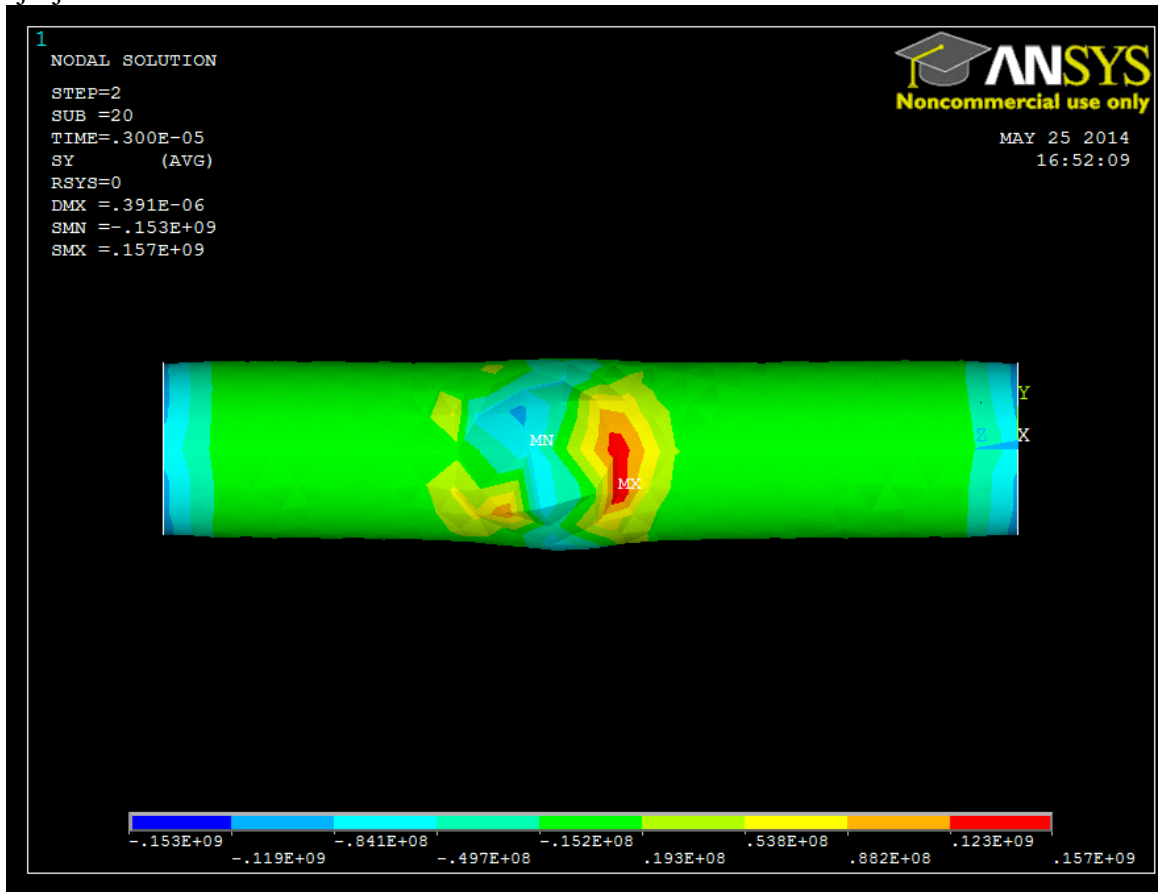


Fig. 29: Thermal Stress in Y-component at $t_{on}=1.82\mu s$

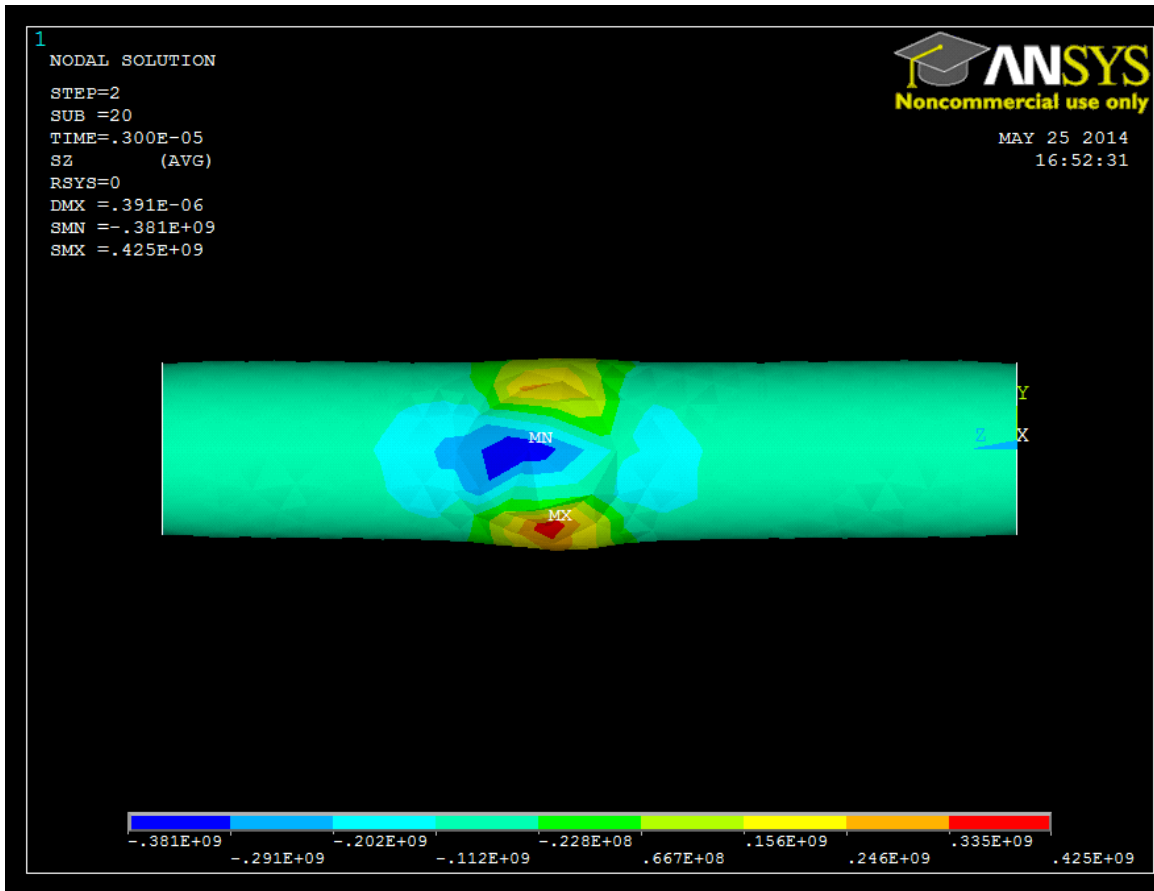


Fig. 30: Thermal Stress in Z-component at $t_{on}=1.82\mu s$

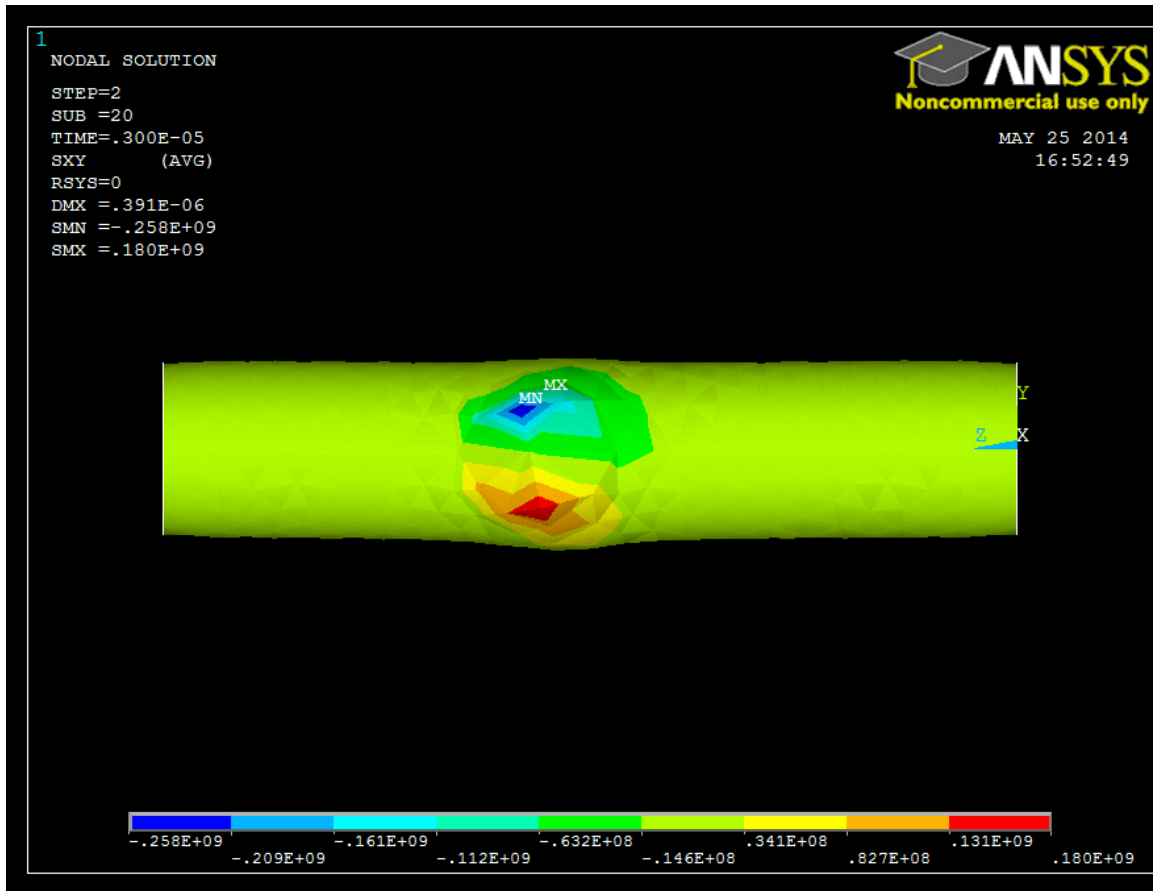


Fig. 31: Thermal Stress in XY-component at $t_{on}=1.82\mu s$

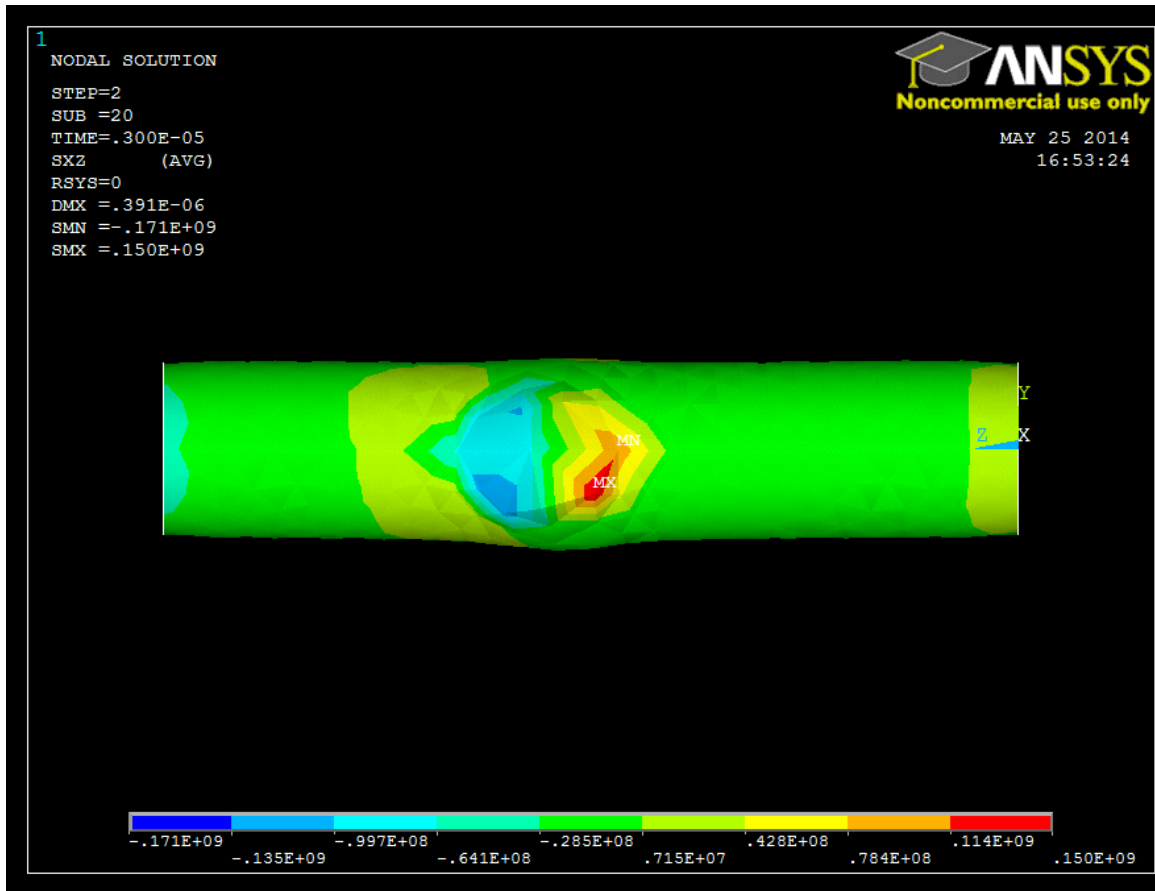


Fig. 32: Thermal Stress in XZ-component at $t_{on}=1.82\mu s$

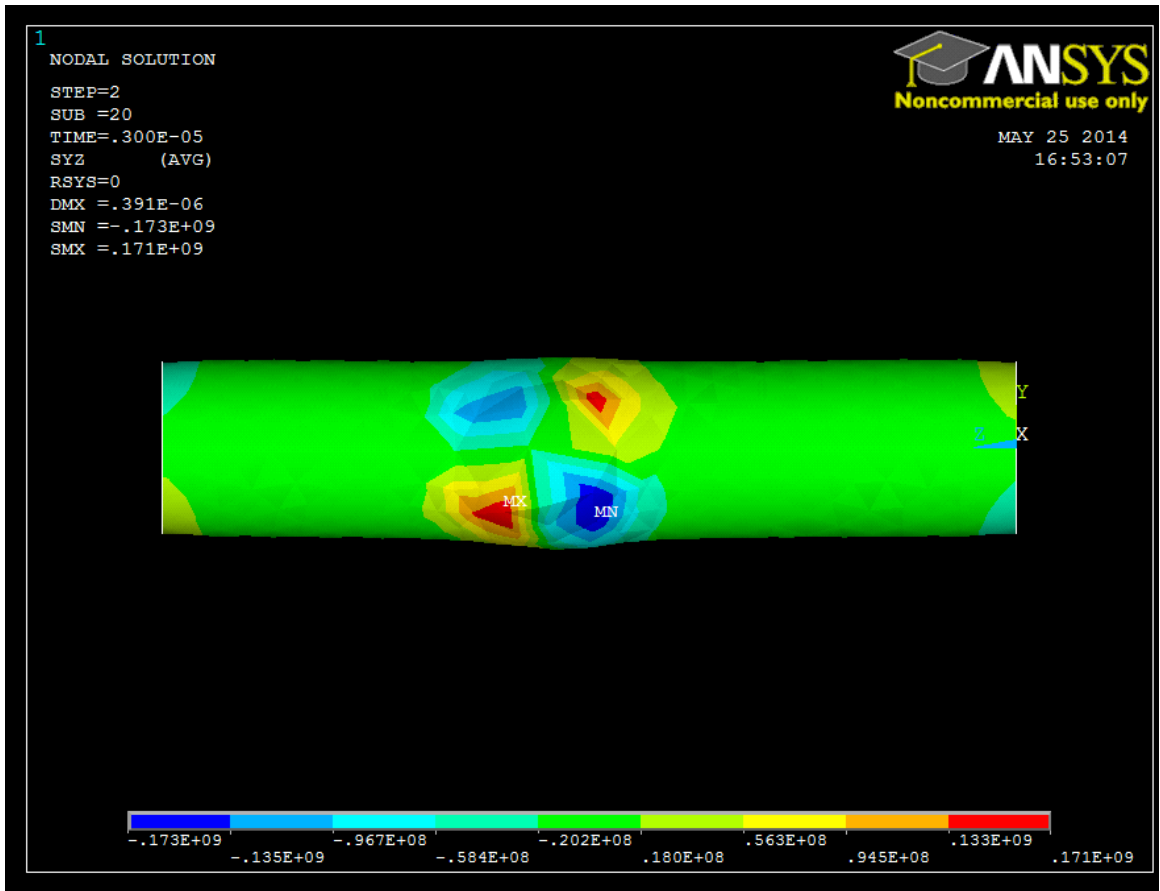


Fig. 33: Thermal Stress in YZ-component at $t_{on}=1.82\mu s$

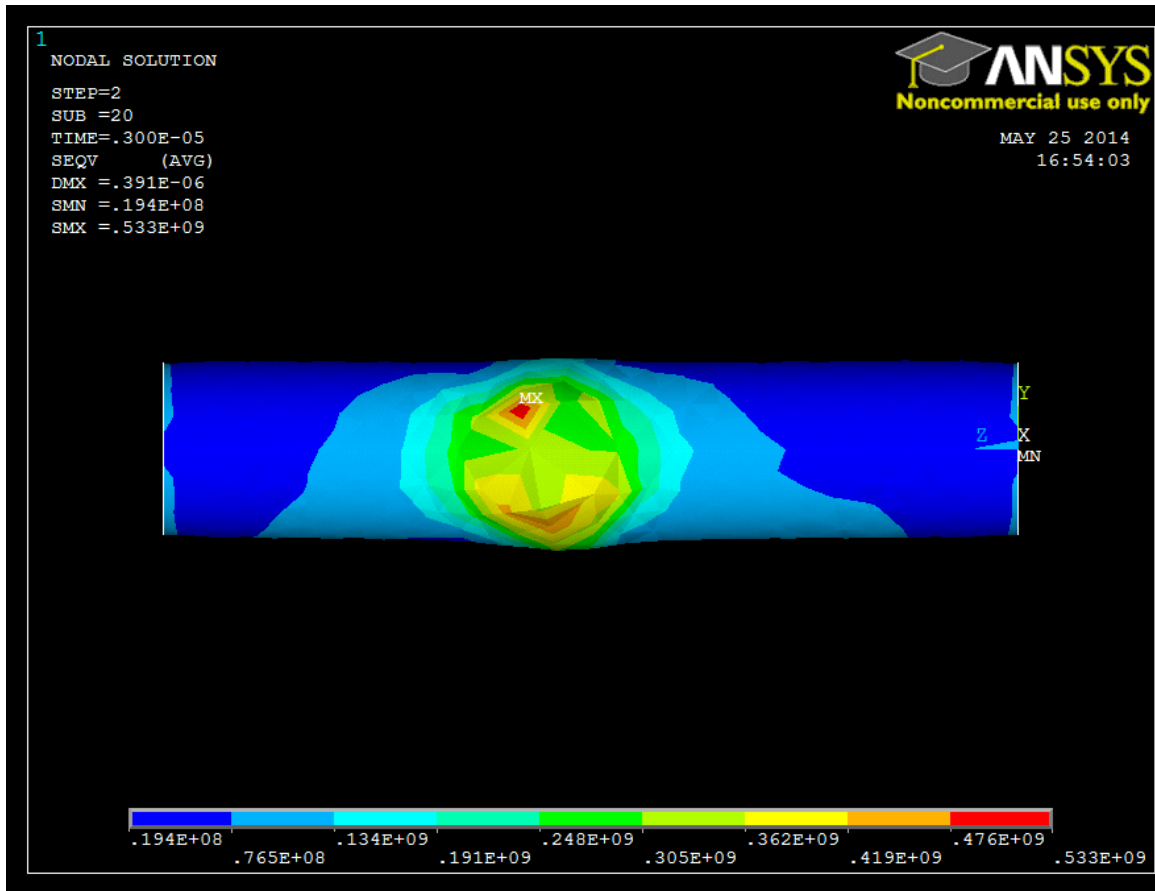


Fig.34: Residual stress at $t_{\text{off}}= 3 \mu\text{s}$

4.3 Results and Discussions

Temperature distributions at the end of the pulse time are shown in Figs.(3- 9) to know the effects on WEDM. The temperature distribution during single discharge is calculated with the energy input constant parameter $I_p= 27$ A, voltage =25V with varying pulse time. At pulse time = 0.12 μ s, corresponding temperature is 86.75⁰C. At pulse time = 0.26 μ s, corresponding temperature is 247.7⁰C. At pulse time = 0.36 μ s, corresponding temperature is 318.6⁰C. At pulse time = 0.52 μ s, corresponding temperature is 446.9⁰C. At pulse time = 0.58 μ s, corresponding temperature is 578.335⁰C. At pulse time = 1.2 μ s, corresponding temperature is 854.8⁰C. At pulse time = 1.82 μ s, corresponding temperature is 1144⁰C. Further increasing the pulse time is not possible because, at temperature 1083⁰C, the brass wire melt.

The distinctive stress distributions in WEDM process, enumerated at the end of heating cycle are presented. Here, Gaussian heat flux distribution is used for the calculation of temperature distribution. Later on, by varying the parameter i.e. pulse duration, and study of thermal stresses are presented. Fig 10-34 shows the thermal stress in different pulse on time. Thermal stress developed after the end of the spark and residual stress developed after subsequent cooling. The nature of the maximum stress is compressive, and it is because during the pulse duration, the heat flux supplied to the tool electrode for a very short duration (in μ s).The maximum compressive stress is 563MPa for $t_{on}=0.12\mu$ s in X-component, and maximum residual stress is 778 MPa. The maximum compressive stress is 288Mpa for $t_{on}=0.52\mu$ s in Z-component and maximum residual stress is 288 MPa. The maximum compressive stress is 425Mpa for $t_{on}=1.82\mu$ s in Z-component and maximum residual stress is 533 MPa.

Chapter 5

- **CONCLUSIONS**

In this dissertation, a robust three dimensional finite element model has been developed using ANSYS software to predict the temperature distribution at different pulse time as well as stress distribution in the wire of WEDM. A transient thermal analysis assuming a Gaussian distribution heat source with temperature-dependent material properties has been used to investigate the temperature distribution and stress distribution. Thermal stress was developed after the end of the spark and also residual stress was developed after subsequent cooling. Finite element modeling was carried out for a single spark with temperature-dependent material properties. Certain parameters such as spark radius, discharge current and discharge duration, the latent heat, the plasma channel radius and Gaussian distribution of heat flux, the percentage of discharge energy transferred to the tool electrode have made this study nearer to real process conditions. The FE model shows that, at pulse time = 0.12 μs , corresponding temperature is 86.75⁰C and maximum residual stress is 778 Mpa. At pulse time = 0.26 μs , corresponding temperature is 247.7⁰C and .At pulse time = 0.36 μs , corresponding temperature is 318.6⁰C. At pulse time = 0.52 μs , corresponding temperature is 446.9⁰C and the maximum compressive stress is 288Mpa in Z-component, and maximum residual stress is 288 Mpa. . At pulse time = 0.58 μs , corresponding temperature is 578.335⁰C. At pulse time = 1.2 μs , corresponding temperature is 854.8⁰C. At pulse time = 1.82 μs , corresponding temperature is 1144⁰C and the maximum compressive stress is 425Mpa for $t_{\text{on}}=1.82\mu\text{s}$ in Z-component, and maximum residual stress is 533 Mpa.

Further increasing the pulse time is not possible because, at temperature 1083⁰C, the brass wire melt.

REFERENCES

- [1] Datta, S. and Mahapatra, S.S. (2010) Modeling, simulation and parametric optimization of wire EDM process using response surface methodology coupled with grey-Taguchi technique, *International Journal of Engineering, Science and Technology*, vol. 2, pp. 162-183.
- [2] Kunieda, K. and Furudate, C. (2001) High Precision Finish Cutting by Dry WEDM, *Journal of Materials Processing Technology*, vol. 149 pp. 77–82
- [3] Okada, O., Uno, Y., Nakazawa, M. and Yamauchi, T. (2010) Evaluations of spark distribution and wire vibration in wire EDM by high-speed. *Manufacturing Technology*, vol.59, pp. 231–234
- [4] Cabanesa, I., Portilloa, E., Marcosa, M. and Sańchezb, J.A. (2 0 0 8) An industrial application for on-line detection of instability and wire breakage in wire EDM, *journal of materials processing technology*, vol. 1 9 5, pp. 101–109
- [5] Saha, S., Pachon, M., Ghoshal, A. and Schulz d, M.J. (2004) Finite element modeling and optimization to prevent wire breakage in electro-discharge machining Mechanics, *Research Communications*, vol. 31, pp. 451–463
- [6] Hou, P.J., Guo, Y.F., Sun, L.X. and Deng G.Q. (2 0 1 3) Simulation of temperature and thermal stress filed during reciprocating traveling WEDM of insulating ceramics, *Procedia CIRP* vol. 6 PP. 410 – 415
- [7] Hada, K. and Kunieda, M. (2013) Analysis of wire impedance in wire-EDM considering Electromagnetic fields generated around wire electrode, *Procedia CIRP* vol.6 245 – 250

- [8] Cabanesa, I., Portilloa, E., Marcosa, M. and Sa´nchezb, J.A. (2 0 0 8) On-line prevention of wire breakage in wire electro-discharge machining, *Robotics and Computer-Integrated Manufacturing*, vol. 24, pp. 287-289.
- [9] Cheng, G., Zhijing, H. and Feng (2007) Experimental determination of convective heat transfer coefficient in WEDM, *International Journal of Machine Tools & Manufacture*, vol. 47, pp. 1744–1751
- [10] Yan, M.T. and Lai, Y.P. (2007) Surface quality improvement of wire-EDM using a fine-finish power supply, *International Journal of Machine Tools & Manufacture*, vol.47, pp. 1686–1694
- [11] Yuana, J., Wangb, K., Yua, T. and Fanga, M. (2008) Reliable multi-objective optimization of high-speed WEDM process based on Gaussian process regression, *International Journal of Machine Tools & Manufacture*, vol. 48, pp. 47–60
- [12] Hana, F., Chenga, G., Fenga, Z. and Isagoc, S. (2008) Thermo-mechanical analysis and optimal tension control of micro wire electrode, *International Journal of Machine Tools & Manufacture*, vol. 48, pp. 922–931
- [13] Sanchez, J.A., Plaza, S., Ortega, N. Marcos, M. and Alizarin, J. (2008) Experimental and numerical study of angular error in wire-EDM taper-cutting, *International Journal of Machine Tools & Manufacture*, vol. 48, pp. 1420– 1428
- [14] Izquierdo, B., Sa, J.A., nchez, Plaza, S., Pombo, I., Ortega, N. (2009) A numerical model of the EDM process considering the effect of multiple discharges. *International Journal of Machine Tools & Manufacture*, vol. 49, pp. 220–229.

- [15] Shichun, Di. Xuyang , C., Dongbo, Zhenlong, W. and ChiLiu, Y. (2009) Analysis of kerf width in micro-WEDM, *International Journal of Machine Tools & Manufacture* vol. 49 pp. 788
- [16] Liao Y.S. and Yub, Y.P. (2004) The energy aspect of material property in WEDM and its application. *Journal of Materials Processing Technology* vol. 149 pp. 77–82
- [17] Tani, T., Fukazawa, Y., Mohri , N. Saito, N., Okadaa, M. (2004) Machining phenomena in WEDM of insulating ceramics, *Journal of Materials Processing Technology* vol. 149 pp. 124–128
- [18] Alias, A., Abdullaha , B. and Mohd, A (2012) Influence of machine feed rate in WEDM of titanium Ti-6Al-4V with constant current (6A) using brass wire, *Procedia Engineering*, vol. 41 pp. 1806 – 1811.
- [19] Dodun, O., Slătineanu and Lorelei, G. (2014) Improving the WEDM process acting on the tool electrode. *Procedia Technology*, vol. 12 pp. 427 – 432

